Aus dem Institut für Funktionelle Anatomie
der Medizinischen Fakultät Charité – Universitätsmedizin Berlin

DISSERTATION

Verteilung von Connexin 43 in der Säugerniere und seine Bedeutung bei der myogenen Transformation renomedullärer Fibroblasten

Distribution of connexin 43 in rodent kidney and its role in myogenic transformation of renal medullary fibroblasts

zur Erlangung des akademischen Grades
Doctor medicinae (Dr. med.)

vorgelegt der Medizinischen Fakultät
Charité – Universitätsmedizin Berlin

von
Yan Xu
aus Jiangsu/China

Datum der Promotion: December 3rd, 2021

Table of Contents

List of abbreviations

AQP	aquaporin
α-SMA	α-smooth muscle actin
BSA	bovine serum albumin
BW	body weight
CD31	cluster of differentiation 31
CKD	chronic kidney diseases
Col1A1	collagen type I-a1
COX-2	cyclooxygenase 2
Cx	connexin
DAPI	4',6-diamidino-2-phenylindole
EGM	extraglomerular mesangium
GA	glutaraldehyde
GAPDH	glyceraldehyde 3-phosphate dehydrogenase
GJ	gap junction
GJIC	gap junctional intercellular communication
IF	immunofluorescence
IGM	intraglomerular mesangium
LY	Lucifer yellow
PBS	phosphate-buffered saline
PFA	paraformaldehyde
RT	room temperature
SL-DT	scalpel loading-fluorescent dye transfer
TEM	transmission electron microscopy
TGF-β1	transformation growth factor-beta1
TGN46	trans-Golgi network 46
TK 173 cell line	cultured human renal medullary fibroblasts
ZO-1	zonula occludens-1
18β-GA	18β-glycyrrhetinic acid

1. Abstract

1.1 Abstract (English)

Connexin 43 (Cx43), a gap junction-forming protein, is widely expressed in the mammalian kidney. Gap junctions mediate the intercellular passage of small molecules < 1 kDa in size. This was found to play critical roles in the maintenance of renal homeostasis and the development of renal pathology. Since previous reports on the cellular distribution of Cx43 have been conflicting, we have studied localization of Cx43 in rat and mouse kidney using confocal immunofluorescence and ultrastructural immunolabelling. In addition, a cultured human renal medullary fibroblast line (TK 173) served to investigate the role of Cx43-composed gap junctions in transforming growth factor-beta1 (TGF-β1)-induced transformation to a myofibroblast phenotype.

Cx43 was abundantly detected in endothelia of renal arteries, arterioles, peritubular capillaries, and descending vasa recta where it was partially colocalized with the endothelial marker CD31. The endothelial cells of lymphatic vessels also expressed Cx43. Substantial Cx43 signals were detected in both extra- and intraglomerular mesangium. As a novel finding, Cx43 was revealed to be expressed substantially in medullary fibroblasts. In the inner medulla, Cx43-positive fibroblasts co-expressed cyclooxygenase-2, and chains of punctate Cx43 signals near the basement membrane of renal tubules and capillaries were assigned to cell processes of fibroblasts. Ultrastructural investigation revealed Cx43 distribution in gap junctional plaques between fibroblasts and between their cell processes. Cultured TK 173 cells expressed Cx43 both in the perinuclear compartment and in the plasma membrane of adjacent cells. Lucifer yellow signal was shown to spread across adjacent cells. Upon application of the gap junction inhibitor, 18β-glycyrrhetinic acid (18β-GA), the spreading was blunted suggesting effective intercellular exchange via functional gap junctions. TGF-β1 induced transformation of the cells into myofibroblasts. Here, α-smooth muscle actin and collagen type I-a1 expression as well as Cx43 biosynthesis and gap junctional Lucifer yellow exchange were enhanced. The application of 18β-GA reversed the profibrotic effect of TGF-β1, suggesting that gap junctional channels composed of Cx43 facilitate transduction of profibrotic signaling between inner medullary fibroblasts.

In sum, our results showed the distribution of Cx43 in renal vasculature, mesangium, and medullary fibroblasts, and its absence from tubular epithelia. Myogenic transformation of

medullary fibroblasts depended on Cx43-mediated information transfer. Addressing renal interstitial fibrosis, a potential role for Cx43 has been outlined.

1.2 Abstract (Deutsch)

Das Gap junction Protein Connexin 43 (Cx43) hat eine weite Verbreitung in Geweben der Säugerniere. Gap junctions erlauben die interzelluläre Passage von Molekülen < 1 kDa. Sie spielen eine wichtige Rolle in physiologischen und pathophysiologischen Prozessen. Da frühere Darstellungen der zellulären Verteilung von Cx43 widersprüchlich waren, wurde diese erneut mittels konfokaler Immunhistochemie und ultrastruktureller Immunmarkierung untersucht. Weiterhin wurde eine Zelllinie aus Fibroblasten des menschlichen Nierenmarks (TK173) als *in vitro* Modell eingesetzt, um die Funktion von Cx43 Gap junctions bei Transforming growth factor-beta1 (TGF-β1)-induzierter Transformation der Zellen zu einem myofibroblastischen Phänotyp zu untersuchen. Das Vorkommen von Cx43 wurde in den CD31-positiven Endothelien renaler Arterien, Arteriolen, peritubulärer Kapillaren und aufsteigender Vasa recta lokalisiert. Lymphatische Gefässendothelien exprimierten ebenfalls Cx43. Deutliche Signale wurden weiterhin im intra- und extraglomerulären Mesangium detektiert. Im Interstitium wurde Cx43 in medullären Fibroblasten nachgewiesen. Diese koeprimierten Cx43 und Cyclooxygenase-2 im inneren Mark. Hier fielen Cx43 Signale als zahlreiche einzelne Gap junctions oder Punkteketten im Konfokalbild auf. Diese wurden an Zellfortsätzen der Fibroblasten identifiziert. Mit ultrastruktureller Immunmarkierung wurde Cx43 an Membran-Kontaktzonen zwischen medullären Fibroblasten und ihren Zellfortsätzen lokalisiert. TK 173 Zellen exprimierten Cx43 perinukleär und in der Plasmamembran. Die Applikation von fluoreszierendem Lucifer yellow-Farbstoff breitete sich in benachbarten Zellen aus. Der Gap junction Inhibitor, 18β-Glycyrretinsäure (18β-GA) verhinderte diese Ausbreitung. Dies zeigte die Gap junction-spezifische Natur der Signalausbreitung. TGF-β1 verursachte die Transformation der Zellen zu Myofibroblasten. Die Expression von glattmuskulärem Aktin (α-SMA) und Collagen 1A1 sowie Cx43 Biosynthese und Gap junction-vermittelte Lucifer yellow-Ausbreitung waren unter TGF-β1 erhöht. Die Gabe von 18β-GA verhinderte diesen profibrotischen Effekt von TGF-β1. Diese Daten weisen darauf hin, dass Cx43 Gap junctions die Koordination profibrotischer Signalwege zwischen innermedullären Fibroblasten koordinieren können.

Unsere Ergebnisse zeigen die Verteilung von Cx43 Gap junctions in Gefäßen, Mesangium und medullären Fibroblasten der Niere sowie ihre Abwesenheit in tubulären Epithelien. Die myogene Transformation medullärer Fibroblasten beruht auf Cx43-vermitteltem Informationsaustausch. Eine Bedeutung der Cx43 Gap junctions bei der Entstehung der Nierenfibrose wird vorgestellt.

2. Introduction

2.1 Connexins and gap junctions

The connexin (Cx) family of proteins comprises membrane-spanning proteins with four transmembrane domains connected by two extracellular loops, a cytoplasmic loop and cytoplasmic N- and C-termini.[1] Until now, 21 Cx isoforms have been found to be expressed in humans. They have been classified by a numerical suffix based on their molecular weight.[1] Six Cx proteins either composed of the same (homomeric) or different (heteromeric) isoforms are organized as hexameric structures with a central pore, termed connexon or hemichannel.[1,2] After trafficking to the cell membrane by microtubules, connexons may form intercellular gap junctions (GJ) by docking to connexons from the adjacent cell. Gap junctions distribute in adjacent, closely apposed parts of plasma membranes from neighboring cells. Here, they provide channels for efficient intercellular communication, a critical step for the functional coordination in multicellular organisms.[3] Ions, metabolites, second messengers, and microRNAs with a molecular weight < 1 kDa can be exchanged through gap junctions between neighboring cells.[3] Gap junctions participate in multiple physiological processes within organs including propagation of electrical activity,[4] cell growth and differentiation, angiogenesis, and immune modulation.[3] Many congenital diseases of auditory, cardiovascular, or musculoskeletal systems have been attributed to mutations in connexin genes.[1] Acquired or genetically induced pathological conditions have been shown to induce dysregulation of the distribution and/or function of gap junctions.[1] Connexins were recently found to participate in other forms of intercellular communication including extracellular vesicles and tunnelling nanotubes.[5,6] Crosstalk between non-opposed cells and, via extracellular vesicles, even between different organs has been shown to depend on connexin channels.[3]

2.2 Cx43 and the kidney

Connexins are extensively expressed in various tissues and organs with functional and spatial heterogeneity.[1] Among the main Cxs in the kidney, Cx37, Cx40, Cx43, and Cx45 were mostly detected in the blood vessels and glomeruli, whereas Cx30, Cx30.3, Cx32, and Cx37 were expressed in various tubule segments.[7] Cx43 is currently the best-characterized Cx whose localization and function in the heart has been well identified, where it principally distributes within intercalated discs, specialized plasma membrane between neighboring cardiomyocytes.[4] Phosphorylation at the C-terminus of Cx43

including 19 serine residues and two tyrosine residues has a significant impact on gap junctional intercellular communication (GJIC), of which Ser368 decreases GJIC by inducing Cx43 internalization.[8] Cx43 is abundantly expressed in the mammalian kidney. Its distribution in endothelia of renal arteries and arterioles in the form of typical gap junctional plaques has been confirmed by several studies.[9-11] In the glomerular mesangium, substantial Cx43 immunoreactivity was detected by immunohistochemistry, and gap junctions were identified at this site by ultrastructural freeze-fracture technology using transmission electron microscopy (TEM).[9,12] Previous studies demonstrated that renal Cx43 is involved in conduction of vasomotion[11,13] as well as in propagation of calcium waves in the juxtaglomerular apparatus.[14] However, distribution of Cx43 in the kidney has not been fully clarified, which limited further investigation of its potential functions. The information on its localization in peritubular capillaries and vascular bundles was scarce.

The presence of Cx43 in renal epithelium has been conflicting. Gap junctions have been detected ultrastructurally between cells of the proximal tubule, but only Cx37 could be localized here.[7,15] Of note, previous freeze-fracture studies on the structure of the mammalian renal inner medulla described gap junctions of variable size and shape between inner medullary fibroblasts.[16,17] We assumed that these fibroblasts express Cx43.

2.3 Investigation in the present study

To clarify the issue, we have performed immunolabelling experiments on paraffin sections and ultrathin sections using three anti-Cx43 antibodies from different suppliers to explore Cx43 distribution in the rat kidney after verification of their antigen specificity. In order to identify distinct renal compartments, corresponding markers such as cluster of differentiation 31 (CD31) for the endothelium, aquaporin 1 (AQP1) for the descending thin limb, aquaporin 2 (AQP2) for the collecting duct, or cyclooxygenase 2 (COX-2) for inner medullary fibroblasts were applied for double labelling with anti-Cx43 antibodies. As a novel finding, we identified Cx43 expression within medullary fibroblasts of rat and mouse kidney. This observation was consistent with finding Cx43 signals in cultured human renal medullary fibroblasts (TK 173) by immunocytochemistry. Early studies on Cx43 function in the kidney mainly focused on its contribution in the control of blood pressure and renal hemodynamics.[18] Recent identification of Cx43 as a novel target for anti-fibrotic therapy

in mouse models of experimental nephropathy[19,20] led us to hypothesize that GJIC between medullary fibroblasts facilitates coordination of interstitial profibrotic signaling during fibrosis. To address this hypothesis, transforming growth factor-beta 1 (TGF-β1), a fibrogenic factor, was applied to induce myogenic transformation of the TK 173 cells, and 18β-glycyrrhetinic acid (18β-GA), a gap junction inhibitor, was used to block GJIC between the cells.

2.4 Significance of the present study

In this study, all four kidney zones from the cortex to the inner medulla have been examined in detail with respect to Cx43 distribution. Our data presented heterogeneous localization of Cx43 in different cell types and renal compartments, suggesting a pleiotropic functional concept for gap junctional coupling in the kidney. Ultrastructural investigation of the inner zone of rat kidney with immunogold labelling identified Cx43 distribution between neighboring fibroblasts and between their cell processes. Furthermore, the in vitro experiments on cultured TK 173 cells shed light on the function of Cx43-gap junctional coupling between medullary interstitial fibroblasts. The blockage of gap junctions inhibited myogenic transformation of the cells induced by TGF-β1, suggesting that Cx43 is a potential therapeutic target for renal interstitial fibrosis. Results substantially contributed to a better understanding of Cx43-gap junctional functions in the kidney, providing insights between basic science and clinical application.

3. Materials and Methods

3.1 Animals and perfusion fixation

Adult male Wistar rats, 200 g body weight (BW) and C57BL/6 mice, 25-35 g BW, each n=5, were housed with free access to diet and water under a light-dark cycle of 12 h at 23°C and 75% humidity in the animal facility of Charité-Universitätsmedizin Berlin. Kidneys of the animals were retrogradely perfusion-fixed using 3% paraformaldehyde (PFA, Merck, Darmstadt, Germany) for morphological evaluation. In brief, animals were first anesthetized with isoflurane for approximately 10 s followed by intraperitoneal administration of Nembutal (0.06 mg/g BW; catalogue no. P3761, Merck). Then the abdominal cavity was opened to expose the abdominal aorta. A catheter was inserted into the abdominal aorta and ligated with a sewing thread. The kidneys were rinsed by perfusion with sucrose dissolved in PBS for 30 s, followed by 3% PFA in 0.1 M sodium cacodylate buffer (pH 7.30) as a fixative for 5 min.[21] The kidneys were taken out for different embedding protocols. Perfusion was performed by Prof. Bachmann.

3.2 Tissue preparation

3.2.1 One kidney form the rats and both kidneys from the mice underwent post-fixation in the same fixative solution used in perfusion overnight at 4°C, followed by rinsing, dehydration, and paraffin infiltration for conventional paraffin embedding.

3.2.2 The other kidney from the rats was processed for plastic embedding and ultrathin sectioning to be evaluated by TEM. The inner medulla was separated and cut into small slices. For Epon 812 embedding, small tissue pieces were immersed in 1.5% PFA, 1.5% glutaraldehyde (GA), and 0.05% picric acid in sodium cacodylate buffer (300 mOsmol adjusted with sucrose) overnight at room temperature for post-fixation.[21] Tissue was then osmicated, dehydrated, and embedded in epoxy resin. For LR White embedding protocol, the kidney pieces were immersed in 0.05% GA in 0.1 M sodium cacodylate buffer (300 mOsmol adjusted with sucrose) overnight for post-fixation and infiltrated in LR White. Ultrathin sections of 70 nm thickness were first acquired by an Ultracut S microtome (Leica, Wetzlar, Germany) and later moved to formvar-coated copper or nickel grids for subsequent TEM inspection.[21] For ultrathin cryosections, small tissue samples were immersed in 0.05% GA overnight for post-fixation, then soaked with sucrose solution (2.3 M) to be shock-frozen in liquid nitrogen-cooled isopentane. Ultrathin cryosections were

cut at 80 nm thickness using a cryoultramicrotome (Leica). Sections were then transferred to formvar-coated nickel grids for subsequent TEM inspection.[21]

3.2.3 Testis tissues from mice harbouring a Sertoli cell-specific Cx43 gene knockout (SCCx43KO) and wild type control mice were a gift by Prof. Ralph Brehm (Institute of Anatomy, Hannover, Germany).[22]

3.2.4 Hearts from perfusion-fixed mice were removed and cut into small pieces and processed for conventional paraffin embedding.

Tissue preparation was performed with the help of a technician.

3.3 Cell culture experiments

TK 173, a human renal medullary fibroblast cell line, was used for *in vitro* studies to investigate the function of Cx43-composed gap junctions (Cx43-GJs) in myogenic transformation induced by TGF-β1. This cell line was provided as a gift by G. Müller (Göttingen, Germany) and has been characterized.[23] Cells were cultivated in 75 cm^2 flasks in DMEM medium (PAN-Biotech, Aidenbach, Germany) with 10% fetal calf serum (ThermoFisher Scientific, Darmstadt, Germany) and 1% penicillin/streptavidin (Sigma-Aldrich) at 37°C, 95% humidity, and 5% CO_2.[21] For morphological evaluation by TEM, cells were grown in cell culture dishes of 10 cm diameter until 100% confluency. Then the cells were fixed with 2.5% GA for 30 min at room temperature (RT), postfixed at 4°C overnight followed by Epon embedding for ultrastructural investigation. For protein analysis and mRNA quantification, cells were prepared in cell culture dishes; for immunocytochemistry, cells were allowed to grow on coverslips in 12-well plates. When 70% confluence was achieved, vehicle (0.05% DMSO, catalog no. A944.1, Roth), TGF-β1 (5 ng/ml, catalog no. T7039, Sigma-Aldrich) and/or 18β-GA (25 µM, catalog no. G10105, Sigma-Aldrich) were used to treat the cells in DMEM medium (serum-free) for 48 h.[21] Cell culture was performed with the help of Duygu Elif Yilmaz. Treatment and experiments of cells were performed by myself.

3.4 Immunohistochemistry

Paraffin-embedded sections (4 µm thickness) of kidneys and hearts served for immunofluorescence (IF). Primary antibodies used in this project are provided in Table 1. Sections were first dewaxed in xylene followed by rehydration in a graded ethanol series (100%, 96%, 80%, 70%). Then sections were boiled in citrate buffer (pH 6.0) for 6 min to

retrieve antigens. To block unspecific bindings, sections were incubated with 5% nonfat dry milk in PBS for 30 min at RT. Then primary antibodies, dissolved in the blocking buffer, were incubated on the tissues overnight at 4°C. Cy2- or Cy3-labeled fluorescent secondary antibodies (Dianova, Hamburg, Germany) were applied for 1 h at RT for signal detection. At the same time, nuclei were counterstained with DAPI. After each antibody incubation, sections were washed with PBS three times (5 min each). At last, sections were mounted with glycerol in PBS (1:9). Sections were observed and photographed in a Zeiss confocal microscopy (LSM5 Exciter, Carl Zeiss, Jena, Germany). Immunohistochemistry on sections was performed by myself.

Table 1. Primary antibodies applied in the present study

Target	Source	Catalog no.	Species, clonality	Dilution (for immunofluorescence, unless stated otherwise)
Connexin 43	Sigma-Aldrich	C6219	Rab pAb	1:400 1:1000 (Western blotting)
Connexin 43	Abcam	ab11370	Rab pAb	1:1000
Connexin 43	Cell Signaling Technology	3512	Rab pAb	1:200
CD31	Santa Cruz	sc-376764	Ms mAb	1:400
COX-2	Santa Cruz	sc-1747	Gt pAb	1:200
AQP1	Abcam	ab9566	Ms mAb	1:500
AQP2	Santa Cruz	sc-9882	Gt pAb	1:1000
ZO-1	Thermo Fisher Scientific	33-9100	Ms mAb	1:400
α-SMA	Sigma-Aldrich	A2547	Ms mAb	1:250
phospho-Cx43 Ser368	Cell Signaling Technology	3511	Rab pAb	1:250
TGN46	Bio-Rad	AHP500G	Shp pAb	1:400
GAPDH	Abcam	ab181602	Rab mAb	1:4000

Rab – rabbit, Ms – mouse, Gt – goat, Shp – sheep.

Table 1 was obtained with permission from Yan Xu et al. 2021, Am J Physiol Renal Physiol, article PMID: 33196322 and is presented with modifications.[21]

3.5 Immunocytochemistry

TK 173 cells were cultured on coverslips for immunocytochemistry. For Cx43, phospho-Cx43 Ser368 (pS368-Cx43), and trans-Golgi network 46 (TGN46) detection, cells were fixed in 4% PFA in PBS; for α-smooth muscle actin (α-SMA) staining, 50% acetone mixed

with 50% methanol was applied for fixation. After PFA fixation, 0.5% saponin in PBS was used for permeabilization for 10 min at RT. Then unspecific bindings were blocked with 3% bovine serum albumin (BSA) in PBS for 30 min at RT. Primary antibodies diluted in blocking buffer were incubated on the coverslips at 4°C overnight, followed by fluorescently labeled secondary antibodies, DAPI, and in some conditions phallodin (catalog no. P2141, Sigma-Aldrich) incubation, each for 1 h at RT. After acetone/methanol fixation for α-SMA, the same procedure was performed except that permeabilization was omitted. The coverslips were mounted with Antifade Mountant (catalog no. P36980, ThermoFisher Scientific). Then they were examined and images were acquired by a fluorescence light microscope (Axio Imager 2, Zeiss, Jena, Germany). ImageJ software (National Institutes of Health) was applied to quantify the intensity of the fluorescent signals. Immunocytochemistry *in vitro* was performed by myself.

3.6 Immunogold labelling

Ultrathin sections made from LR White-embedded tissue or from cryopreserved tissue blocks were used for immunogold labelling. One percent nonfat dry milk in PBS was used to block unspecific bindings. After blocking for 30 min at RT sections were incubated with anti-Cx43 antibody (C6219, 1:50) dissolved in the blocking buffer at 4°C overnight. Then 5 nm colloidal gold particle-coupled goat anti-rabbit IgG (Amersham, Munich, Germany) was applied for 60 min at RT. 2.5% GA in PBS was used to stabilize the bound complex. The sections were then stained with 1% phosphotungstic acid and 5% uranyl acetate to increase contrast. Signals were then examined by a Carl Zeiss EM 906 TEM (Oberkochen, Germany). Immunogold labelling was performed with the help of a technician.

3.7 Western blotting

Cell lysates of TK 173 cells were subjected to immunoblot analysis. Cells were harvested and then homogenized in RIPA buffer (Cell Signaling Technology, Frankfurt am Main, Germany) for 30 min on ice, followed by 10 s sonication.[21] Samples were then centrifugated at 14 x 10^3 g for 10 min to remove cell debris. Measurement of the supernatant protein concentration was conducted using a protein assay reagent kit (ThermoFisher Scientific). Supernatant samples (each 20 µg) were electrophoretically separated by polyacrylamide gels (10%), then transferred to nitrocellulose membranes. After blocking with 5% BSA in PBS, the membranes were incubated with primary antibody

at 4°C overnight. Then peroxidase-conjugated secondary antibodies (DAKO, Hamburg, Germany) were incubated for 1 h at RT. Signal detection was achieved with ChemoCam Imager ECL (Intas, Göttingen, Germany) after chemiluminescence exposure of the membranes. Optical densities of protein bands were assessed with ImageJ software. Western blotting was performed by myself.

3.8 siRNA transfection

For cellular knockdown of Cx43, siRNAs targeting Cx43 (Life Technologies) were transfected into cultured TK 173 cells (30% confluence) for 72 h by INTERFERin (Polyplus transfection, Illkirch, France). The sequence of siRNAs used here is given in Table 2.

3.9 Quantitative RT-PCR

Total RNA was isolated from cultured TK 173 cells using the TRIzol-chloroform method (Promega, Walldorf, Germany). Concentration and quality of the isolated RNA were examined, and then 1 µg of mRNA was reverse-transcribed to cDNA with a reverse-transcriptase kit (Bioline, Luckenwalde, Germany). Specific forward and reverse primers were designed to amplify collagen type I-a1 (Col1A1) and GAPDH (glyceraldehyde-3-phosphate dehydrogenase) (Table 2). Expression level of Col1A1 was normalized against GAPDH. The HOT FIREPol EvaGreen qPCR Mix Plus (Solis BioDyne, Tartu, Estonia) and the 7500 Fast Real-Time PCR system (Applied Biosystems, Darmstadt, Germany) were used for DNA amplification.[21] Results were analyzed using the $\Delta\Delta C_T$ method, and mean values of $\log_2^{(\text{relative quantification})}$ from each group were compared.[21] Quantitative RT-PCR *in vitro* was performed by myself.

Table 2 | cDNA primers and siRNA applied

cDNA primers		
Product	**Forward Primer**	**Reverse Primer**
Col1A1	5'-TCT GCG ACA ACG GCA AGG TG-3'	5'-GAC GCC GGT GGT TTC TTG GT-3'
GAPDH	5' -TGC ACC ACC AAC TGC TTA GC- 3'	5' -GGC ATG GAC TGT GGT CAT GAG- 3'

siRNA		
Target	**Sense**	**Antisense**
Cx43	5' –GUU CAA GUA CGG UAU UGA Att- 3'	5' –UUC AAU ACC GUA CUU GAA Ctt- 3'

Col1A1, Collagen type I-a1; GAPDH, glyceraldehyde 3-phosphate dehydrogenase; Cx43, connexin 43.

3.10 Scalpel loading-fluorescent dye transfer (SL-DT) assay

To perform the SL-DT assay, TK 173 cells were grown on coverslips of 12 mm in diameter placed in 3.5 cm petri dishes. After treatment with vehicle (0.05% DMSO), TGF-β1 (5 ng/ml) and/or 18β-GA (25 μM) for 2 days, cells were washed with PBS three times. Then 2 ml Lucifer yellow (LY, catalog no. L0144, Sigma-Aldrich; 1mg/ml) dissolved in PBS was applied to the dishes, followed by cutting lines through the monolayers by a surgical scalpel to let the dye enter injured cells. LY solution was aspirated after incubation in a dark environment for 10 min, then the cells were rinsed three times with PBS to remove remaining extracellular dye. At last, cells on coverslips were fixed with 4% PFA in PBS for 15 min at RT and mounted with antifade mountant.[21] The coverslips were viewed and photographed with a fluorescence light microscope (Zeiss Axio Imager 2). The area of LY-containing cells was determined with image J as the indicator of GJIC. Then relative LY spread areas were analyzed by dividing the values of the experimental groups by that of the vehicle group as published before.[24] SL-DT assay was performed with the help of Junda Hu.

3.11 Statistical analysis

One-way ANOVA with Tukey's post hoc test was applied to compare data with normal distribution between multiple groups. GraphPad Prism 7.0 as a professional software was used to analyze P values, which < 0.05 was considered statistically significant. All data are expressed as means ± SD. Statistical analysis was performed by myself.

4. Results

4.1 Verification of anti-Cx43 antibodies specificity

Specificity of three antibodies against the C-terminal segment of the cytoplasmic domain of Cx43 from different suppliers was tested in cell lysates of TK 173 cells transfected with the siRNAs targeting Cx43 and in paraffin-embedded testis from mice with conditional Cx43 knockout specifically in the Sertoli cells (SCCx43KO).[22] All of the three antibodies showed the same results, the labelling with the Sigma-Antibody (C6219) was here selected for presentation. The antibody incubation only presented Cx43 bands in cell lysates of the vehicle group, whereas no bands showed up in Cx43-siRNA transfected TK 173 cell lysates (Fig. 1A). Cx43 immunostaining produced clear signals at the blood-testis barrier formed by the Sertoli cells of the seminiferous epithelium in the normal testis (Fig. 1B). No immunoreactivity was found in the SCCx43KO tissue in analogous location (Fig. 1C). Distribution of Cx43 in intercalated discs of myocardium has been established earlier;[7] for further control, immunofluorescence and immunogold labelling with the anti-Cx43 antibody were performed in mouse myocardium. Both procedures revealed prominent Cx43 signals in intercalated discs formed by neighboring cardiomyocytes (Fig. 1, D and E). These results confirmed that the C6219 antibody specifically recognized the Cx43 molecule.

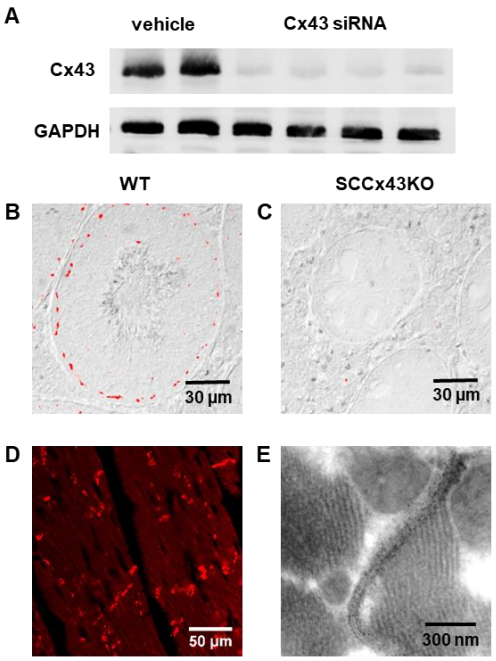

Figure 1. Verification of the C6219 anti-Cx43 antibody specificity. (A) The representative immunoblot shows Cx43 bands in TK 173 cell lysates transfected with vehicle or siRNAs targeting Cx43 for 48 h.

GAPDH serves as the loading control. (B) In the testis from a WT mouse, dotted Cx43 signals (red**)** are localized at the blood-testis barrier shown by the differential interference contrast image. (C) No Cx43 immunoreactivity is detected in testis from a SCCx43KO mouse. (D) Cx43-immunofluorescence (red) is distributed in intercalated discs of WT mouse myocardium. (E) Immunogold labelling shows Cx43 signals in the gap junctional areas between neighboring cardiomyocytes of WT mouse. Figure 1 was obtained with permission from Yan Xu et al. 2021, Am J Physiol Renal Physiol, article PMID: 33196322 and is presented with modifications.[21]

4.2 Cx43 localization in preglomerular vasculature of rat and mouse kidney by immunofluorescence microscopy

In the rat kidney, Cx43 immunofluorescent signals appeared in the endothelia of arcuate and interlobular arteries as well as the afferent arterioles. Single Cx43-fluorescent dots localized between neighboring endothelial cells marked the cell junctions in cross-sectional profiles (Fig. 2A). In the tangential plane, Cx43 signals presented as continuous short lines indicating that intercellular gap junctions were lining the entire length of endothelial cell borders (Fig. 2B). Double-labelling with CD31, an endothelial marker, verified Cx43 distribution in the endothelium, showing partial colocalization of the two molecules (merge images of Fig. 2, A and B). The endothelium of lymphatics accompanying arcuate and interlobular arteries was CD31-negative but expressed Cx43 (arrow in Fig. 2A). The tunica media of vessels showed no Cx43 immunoreactivity throughout. Punctate Cx43 signals were associated with the renin-producing granular cells of the terminal segment of the afferent arterioles (Fig. 2C). Cx43 immunoreactivity showed largely the same distribution pattern in this compartment of the mouse kidney as observed in the rat kidney. Cx43 signal was localized to the endothelium of renal arteries and accompanying lymphatic vessels as well as glomerular arterioles (Fig. 2, D, E, and F).

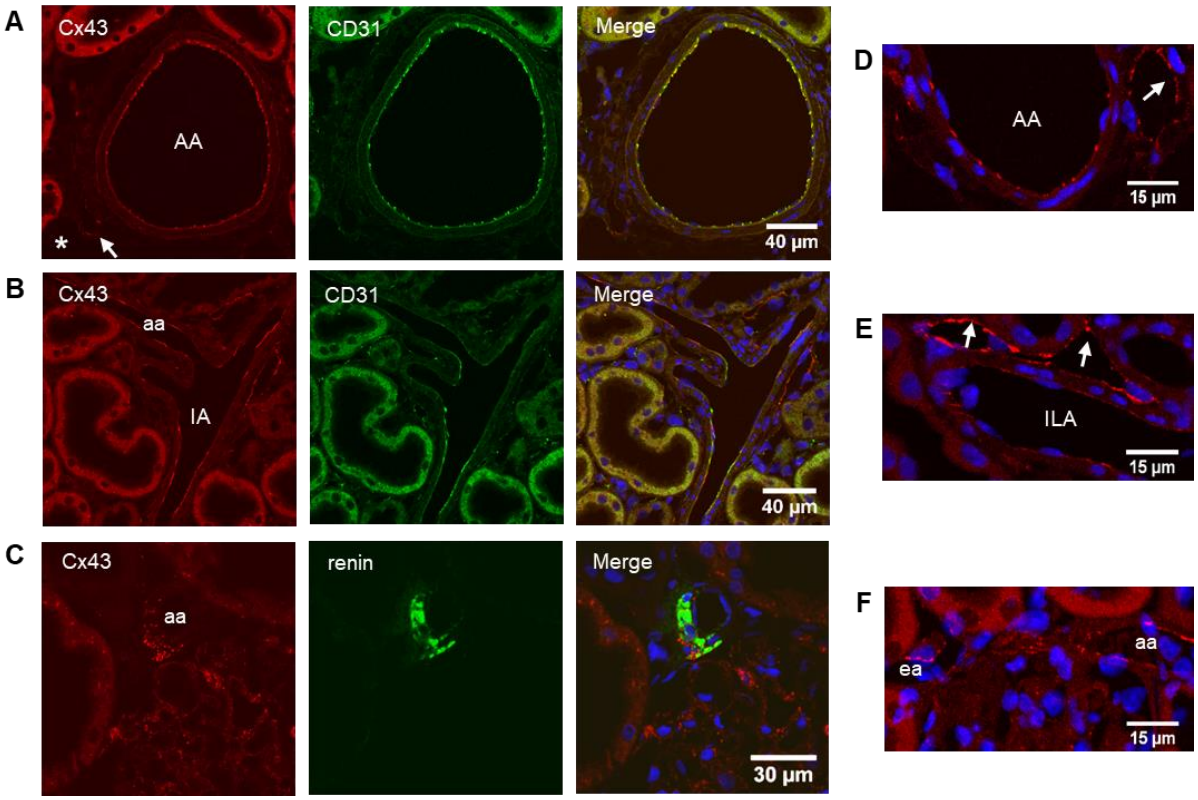

Figure 2. Localization of Cx43 in preglomerular vasculature of rat and mouse kidney. (A) In the cross-sectional profile of an arcuate artery (AA), immunoreactivity of Cx43 shows dotted fluorescence (red) at borders of endothelial cells. The cells also expresses CD31 (green), which partially colocalizes with Cx43 (yellow in the merge image). Anti-Cx43 immunostaining shows endothelial signals in an adjacent lymphatic vessel (arrow) which lacks CD31 expression. The venous endothelium is unreactive for both, Cx43 and CD31 (*). (B) In tangential plane, Cx43 signal (red) is distributed along endothelial cell borders of an interlobular artery (IA) and an afferent arteriole (aa). CD31 signals (green) present a similar pattern but limited colocalization with Cx43 (yellow) in the merge image. (C) Punctate Cx43-immunofluorescent signals (red) at renin-producing cells (green) of the terminal afferent arteriole (aa). (D) Punctate signals of anti-Cx43 at the cell borders of endothelium in a cross-sectional profile of an arcuate artery (AA). Accompanying lymphatic vessel shows endothelial Cx43 signals (arrow). (E) In a tangential plane, Cx43 signals appear at endothelial cell borders of an interlobular artery (ILA). Arrows show Cx43-positive lymphatic endothelium. (F) Cx43-positive endothelia of afferent (aa) and efferent arterioles (ea). In the merge images, nuclei are counterstained with DAPI. A-C show distribution of Cx43 in the rat kidney, and D-F present Cx43 localization in the mouse kidney. Figure 2 was obtained with permission from Yan Xu et al. 2021, Am J Physiol Renal Physiol, article PMID: 33196322 and is presented with modifications.[21]

4.3 Cx43 localization in mesangium of rat and mouse kidney by immunofluorescence microscopy

In the extraglomerular mesangium of the rat kidney, a high density of Cx43-fluorescent dots was detected (EGM, Fig. 3A). Cells continuing into the intraglomerular mesangium

(IGM) also expressed Cx43, although in lesser density, demonstrating functional links between EGM and the glomerular tuft (Fig. 3A). There was no colocalization of Cx43 with CD31 in the glomerular tuft, since glomerular capillaries were Cx43-negative (Fig. 3B). No Cx43 immunoreactivity (Fig. 3B) was detected in podocytes and parietal epithelia. Cx43 signals were also observed in both extra- and intraglomerular mesangium of the mouse kidney as fluorescent dots between mesangial cells (Fig. 3C).

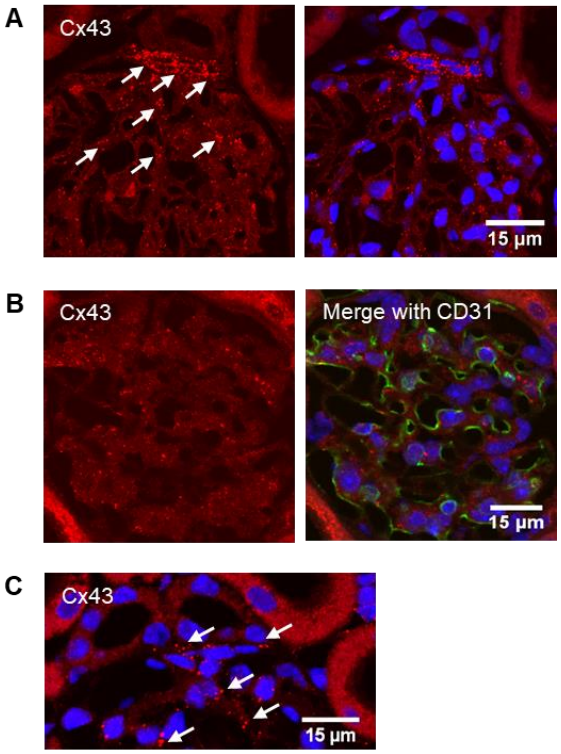

Figure 3. Localization of Cx43 in mesangium of rat and mouse kidney. (A) Substantial Cx43-positive dots (arrows) between extraglomerular mesangial cells, continuing into the intraglomerular mesangium of the rat kidney. (B) No co-localization of Cx43 and the endothelial marker CD31 in the glomerulus of the rat kidney. (C) Cx43-fluorescent dots (arrows) in extra- and intraglomerular mesangium of the mouse kidney. In the merge images, nuclei are counterstained with DAPI. Figure 3 was obtained with permission from Yan Xu et al. 2021, Am J Physiol Renal Physiol, article PMID: 33196322 and is presented with modifications.[21]

4.4 Cx43 localization in postglomerular vasculature of rat and mouse kidney by immunofluorescence microscopy

In the cortical interstitium of the rat kidney, Cx43 signals were localized in the endothelium of peritubular capillaries, which was also positive for CD31 (Fig. 4A). Cx43 immunoreactivity was further detected along endothelial cells borders of the descending vasa recta, whereas no Cx43 signals were detected in the ascending vasa recta of outer

medulla (Fig. 4, B and C). Endothelia of descending and ascending vasa recta were CD31 positive; where coexpressed, Cx43 and CD31 signals did not exactly overlap (merge images in Fig. 4, B and C). In the inner medulla, punctate Cx43 signals were detected near the basement membrane of collecting ducts. Here, signals were not related with endothelial cells of the capillaries, which was only CD31-positive (Fig. 4D).

Similar to the rat kidney, Cx43 was localized to the endothelium of peritubular capillaries (Fig. 4E) of the cortex and descending vasa recta of outer medulla (Fig. 4F) in postglomerular vasculature of the mouse kidney, while ascending vasa recta of the outer medulla and inner medullary capillaries were Cx43-negative.

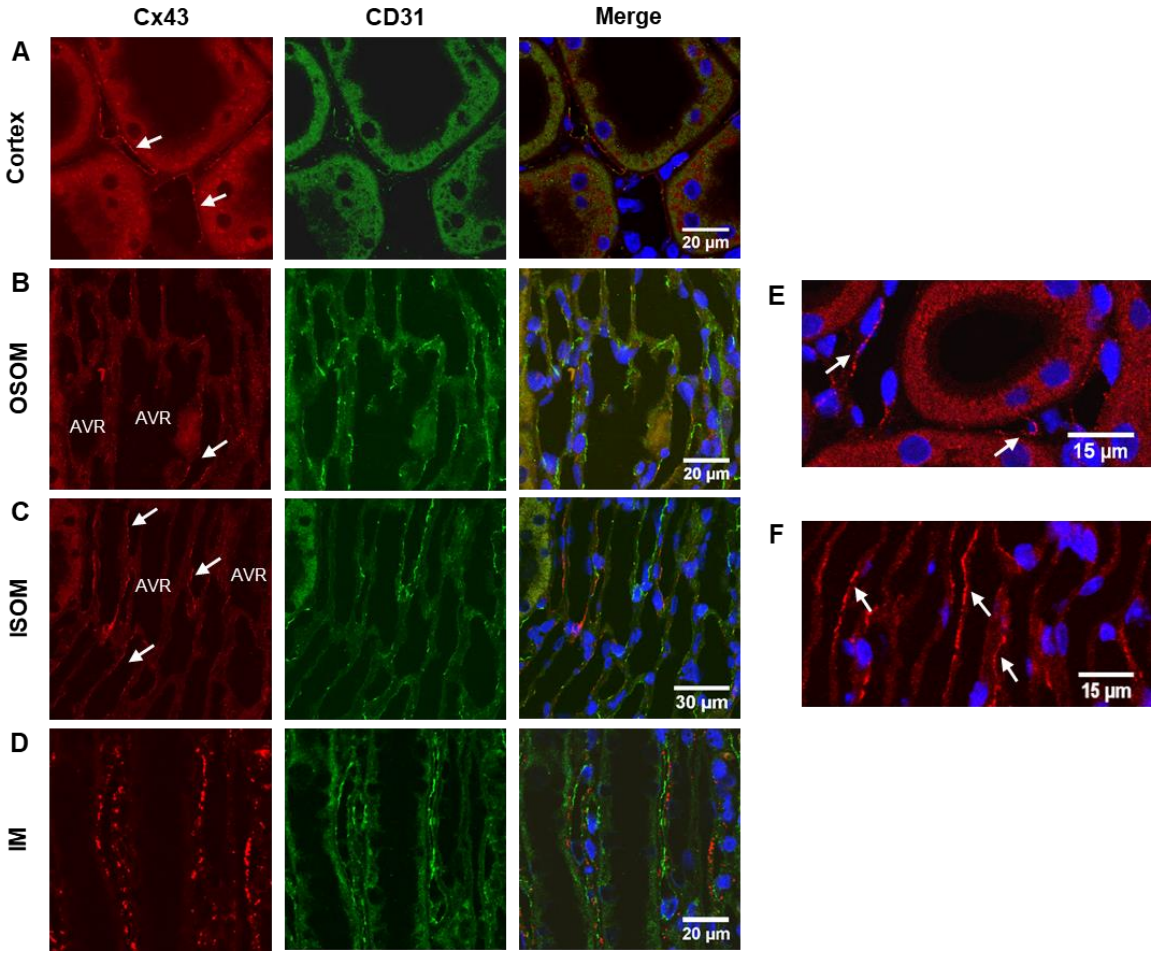

Figure 4. Localization of Cx43 in postglomerular vasculature of rat and mouse kidney. (A) In the cortex, Cx43-immunoreactive signals (red, arrows) display continuous lines within endothelia of peritubular capillaries, which are also CD31 positive (green). (B) In vascular bundles of OSOM, endothelia of the vasa recta are CD31 positive (green), while only the endothelia of descending vasa recta express Cx43 (red, arrow). (C) In vascular bundles of ISOM, endothelia of descending but not ascending vasa recta (AVR) contain Cx43 signals (red, arrows). (D) In the inner medulla (IM), dotted Cx43-immunoreactive chains (red) are located between epithelia and CD31-positive endothelia of vasa recta or capillaries (green). Cx43 and

CD31 signals are not colocalized as shown in the merge image. In the merge images, nuclei are counterstained with DAPI. (E) Continuous Cx43 staining (arrows) along cortical peritubular capillaries. (F) Cx43-positive descending vasa recta in vascular bundles of the outer medulla (arrows). A-D show distribution of Cx43 in the rat kidney. E and F present Cx43 localization in the mouse kidney. Figure 4 was obtained with permission from Yan Xu et al. 2021, Am J Physiol Renal Physiol, article PMID: 33196322 and is presented with modifications.[21]

4.5 Cx43 expression by medullary interstitial cells of rat and mouse kidney by immunofluorescence microscopy

In rat and mouse kidney, immunolabelling of Cx43 also displayed significant signals in interstitial fibroblasts of the renal medulla, whereas cortical fibroblasts showed no Cx43 immunoreactivity. In the outer medulla, Cx43 immunoreactivity was localized in the perinuclear compartment of fibroblasts and in their cell processes (Fig. 5, A, B, and D). By contrast, Cx43 distributed as two different patterns in the inner medulla. One kind presented as comma-like signals in the perinuclear region of fibroblasts, and the other kind appeared as chains of fluorescent puncta near the basement membrane of epithelium and capillaries (Fig. 5, C and E).

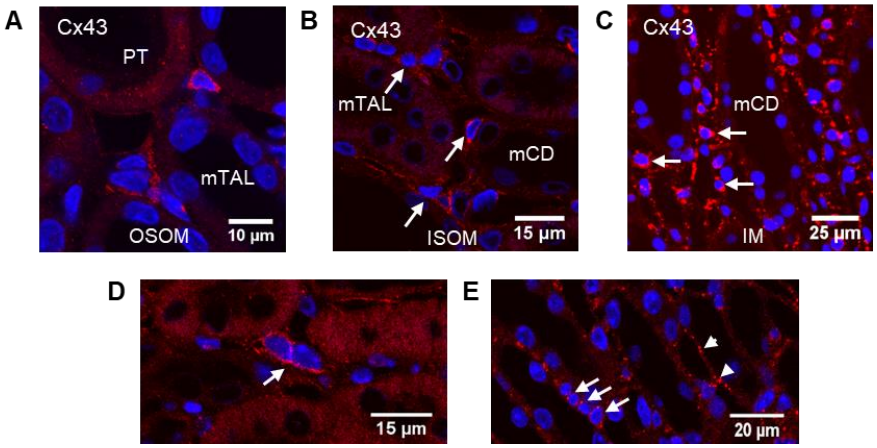

Figure 5. Localization of Cx43 in interstitial cells of rat and mouse kidney. (A) Perinuclear Cx43 signals extending into cell processes (red) of interstitial cells in OSOM of the rat kidney. (B) Perinuclear Cx43 signals extending into cell processes (red, arrows) of interstitial cells in ISOM of the rat kidney. (C) Intracellular Cx43 signals of interstitial cells (red, arrows) and chains of fluorescent red dots between epithelia and vessels in IM of the rat kidney. (D) Interstitial cells in the outer medulla of the mouse kidney (arrow) are Cx43-positive. (E) In the inner medulla of the mouse kidney, Cx43-fluorescent dots mark gap junctions (arrowheads) in the interstitium and Cx43 signals locate in the perinuclear compartments of fibroblasts (arrows). Nuclei are counterstained with DAPI. Figure 5 was obtained with permission from Yan Xu et al. 2021, Am J Physiol Renal Physiol, article PMID: 33196322 and is presented with modifications.[21]

To obtain more detailed information on the inner medullary interstitial distribution of Cx43, double immunostaining experiments were performed. Cells with perinuclear Cx43 signals were recognized as fibroblasts by the co-expression of cyclooxygenase-2 (COX-2) characterizing lipid-laden fibroblasts of renal inner medulla (Fig. 6A). Cx43 was not colocalized with AQP1 in descending thin limbs (Fig. 6B), AQP2 in collecting ducts (Fig. 6C), or zonula occludens-1 (ZO-1) in tight junctions of renal epithelia and endothelia (Fig. 6D). The results from double staining experiments also confirmed that rows of inner medullary Cx43 signals belonged to the cell processes of interstitial fibroblasts. Renal tubular epithelia were all negative for Cx43 from Bowman's capsule all the way to collecting ducts in the renal papilla. No Cx43 expression was found in renal veins either.

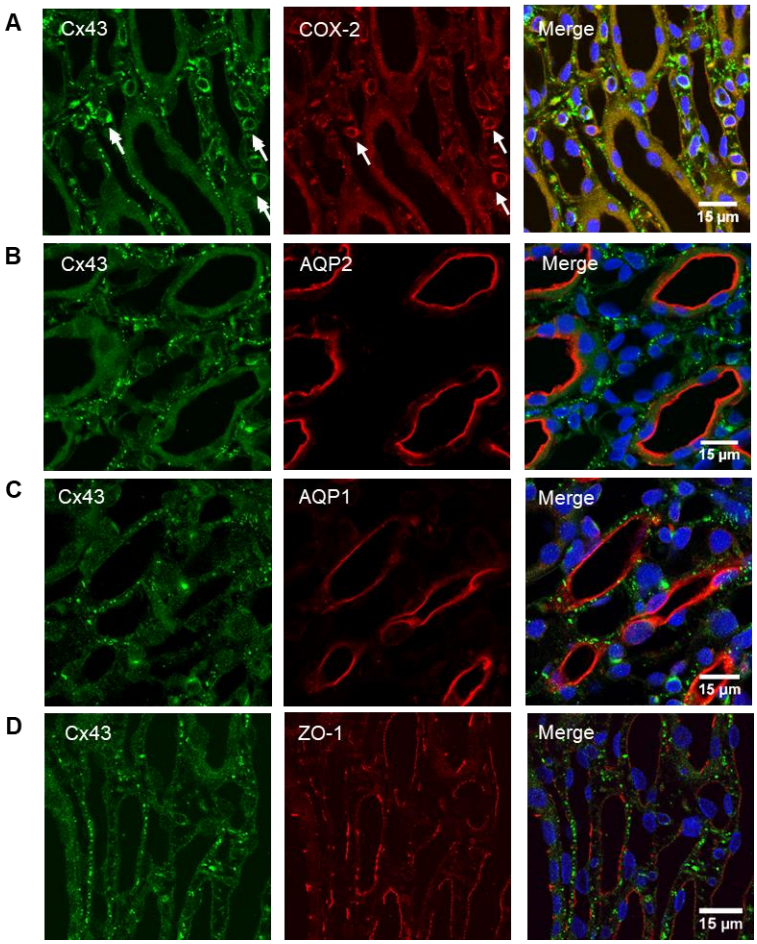

Figure 6. Localization of Cx43 in inner medullary interstitium of the rat kidney. (A) In the IM, perinuclear signals of Cx43 (green) locate in fibroblasts are double-stained with anti-COX-2 (red, arrows). (B) Dotted signals of anti-Cx43 (green) are distributed near medullary collecting ducts identified by anti-AQP2 (red). (C) Chains of Cx43 fluorescent dots (green) located next to inner medullary descending thin limbs labelled with anti-AQP1 (red). (D) There is no colocalization of anti-Cx43 signals (green) with ZO-1

(red), a tight junctional protein expressed in epithelia and endothelia. In the merge images, nuclei are counterstained with DAPI.

4.6 Ultrastructural Cx43 immunolabelling in inner medulla of the rat kidney

In order to further characterize the identity of Cx43-positive cells and the sites of punctate Cx43 signals in the interstitium of renal inner medulla, ultrastructural examination by TEM was conducted. In Epon-embedded ultrathin sections, interstitial fibroblasts were identified by cytosolic lipid droplets. The typical structure of gap junctions as close appositions of parallel plasma membrane portions were observed between cell bodies of adjacent fibroblasts or their cell processes, whose length is between 350 to 700 nm (Fig. 7A). Occasionally, gap junctions were structurally associated with intermediate junctions (Fig. 7A). Immunogold staining on ultrathin cryosections revealed Cx43 signals in gap junctional plaques between cell bodies of neighboring fibroblasts (Fig. 7B). On LR White-embedded ultrathin sections, Cx43 immunogold signals were further detected along gap junctions between individual cell processes of fibroblasts (Fig. 7C). Signals were also found in “reflexive gap junctions” formed by interaction of cell membranes from the same fibroblast (Fig. 7D) as defined earlier.[17]

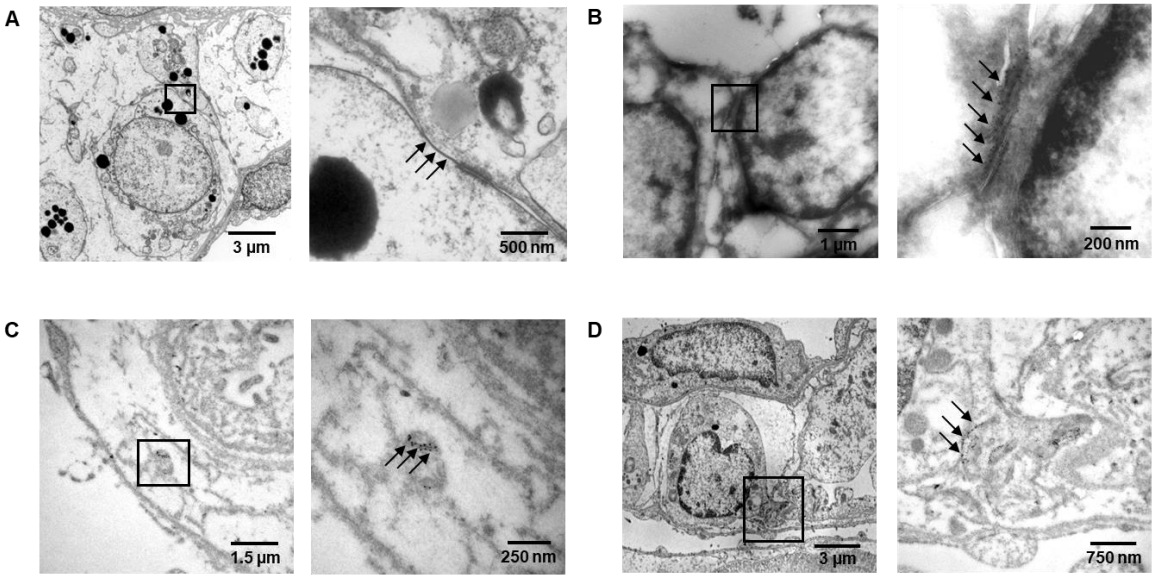

Figure 7. Gap junctions and Cx43 distribution in renal IM of rats with TEM. (A) Typical gap junction structure between two neighboring fibroblasts with characteristic lipid granules (arrows), Epon-embedded ultrathin section. (B) and (C) Immunogold labelling of ultrathin cyrosection (B) and LR-White ultrathin (C) section show Cx43 signals in gap junctional plaques between two adjacent fibroblasts and between cell processes of fibroblasts, respectively (shown by arrows). (D) Cx43 immunogold-positive signals in a reflexive gap junction (arrows), LR-White ultrathin section. Inserts in the left panels correspond to high-

resolution magnifications in the right images. Figure 7 was obtained with permission from Yan Xu et al. 2021, Am J Physiol Renal Physiol, article PMID: 33196322 and is presented with modifications.[21]

4.7 Cx43 expression in cultured human renal fibroblasts

Based on significant Cx43 expression in fibroblasts of renal medulla, the cultured human renal medullary fibroblast (TK 173 cell line) served as an *in vitro* model to investigate the potential function of Cx43-GJs. Cx43 and pCx43 S368 were localized in this cell line by immunocytochemistry. Similar to the *in vivo* findings, immunolabelling of Cx43 displayed two different patterns of distribution. Dotted immunofluorescent Cx43 signals were found in gap junctional plaques between neighboring fibroblasts, and significant intracellular Cx43 immunoreactivity was also localized in the perinuclear compartment (Fig. 8A). Intracellular Cx43 signals showed minor overlap with the marker of the trans-Golgi network, anti-TGN46 (Fig. 8B), while the non-colocalized portion probably indicated trafficking of Cx43 to the plasma membrane after oligomerization in the Golgi complex. Immunostaining with anti-pCx43 S368 revealed punctate signals at the junctions between adjacent fibroblasts, but no intracellular immunoreactivity (Fig. 8C).

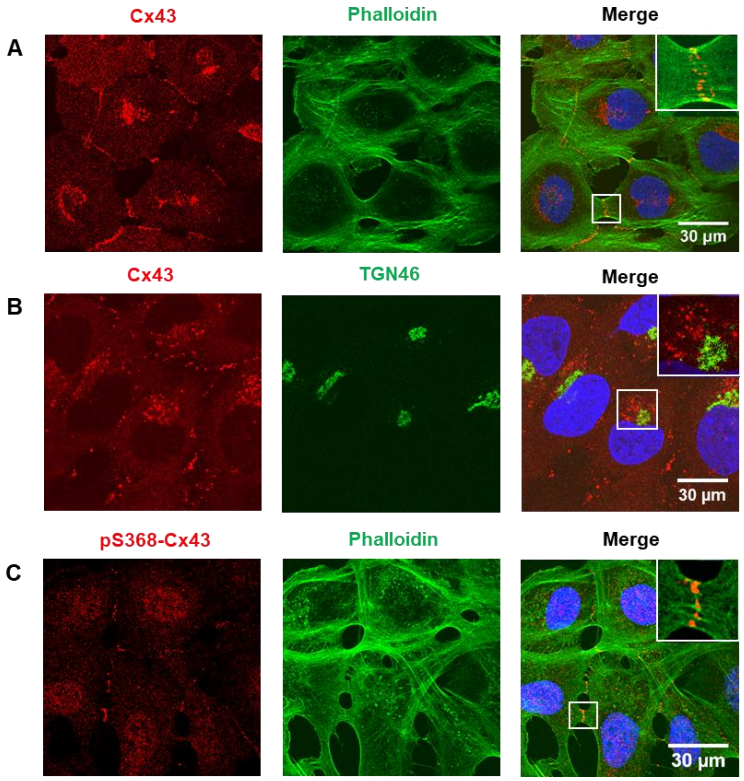

Figure 8. Cx43 expression in cultured human renal medullary fibroblasts (TK 173). (A) Cx43 on plasma membranes between adjacent TK 173 cells represent gap junctions; signal is also in the perinuclear

compartment (red). F-actin is labelled with phalloidin (green). (B) Cx43 signal in the perinuclear compartment is partially associated with the Golgi complex identified by anti-TGN46. (C) Scattered pS368-Cx43 signals on plasma membrane between neighboring TK 173 cells; phalloidin (green)-positive F-actin. Nuclei are counterstained with DAPI (A-C). Figure 8 was obtained with permission from Yan Xu et al. 2021, Am J Physiol Renal Physiol, article PMID: 33196322 and is presented with modifications.[21]

4.8 Functional Cx43-gap junctions between cultured human renal fibroblasts

Firstly, gap junctional plaques were ultrastructurally identified as close apposition of parallel plasma membranes between neighboring cells in TEM (Fig. 9A). With Cx43 established in intercellular gap junctions of TK 173 cells, the SL-DT technique with LY was performed to test intercellular communication mediated by gap junctional coupling. LY migrated for 60 µm in average from the cutting line to distal cells after 10 min incubation, while its migration was abolished after administration of the gap junction inhibitor, 18β-GA (25 µM, Fig. 9B) for 2 h. In the presence of 18β-GA, LY was restricted to the injured cells by cutting (20 µm in average). The result suggested that intercellular spread of the dye was dependent on functional GJs composed of Cx43 located between TK 173 cells.

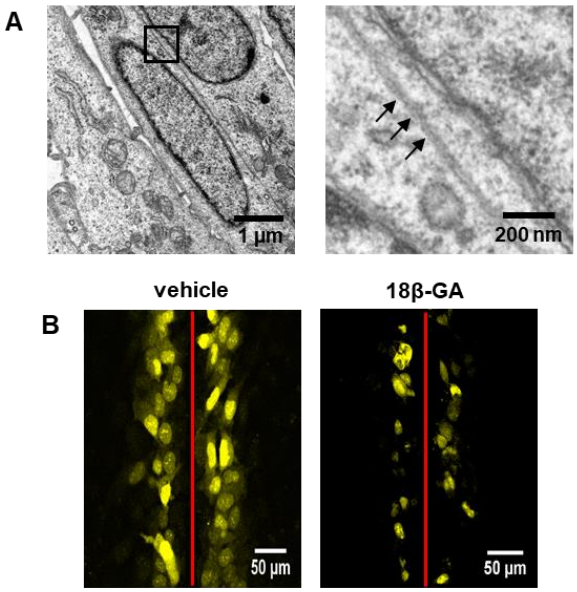

Figure 9. Functional Cx43-gap junctions between cultured human renal medullary fibroblasts (TK 173). (A) Structure of gap junction between neighboring TK 173 cells (shown by arrows), ultrathin Epon section (magnified on the right). (B) Lucifer yellow migrated into cells distal to the cutting line (red) in the vehicle group (left). The spread was blocked by 18β-GA (25 µM, right) for 2 h. Figure 9 was obtained with permission from Yan Xu et al. 2021, Am J Physiol Renal Physiol, article PMID: 33196322 and is presented with modifications.[21]

4.9 Cx43 expression and gap junction-mediated communication are upregulated by TGF-β1

Consistent with previous studies,[25] Cx43 in TK 173 cells presented three bands by Western blotting. The non-phosphorylated form (Cx43-NP), the phosphorylated form 1 (Cx43-P1), and the phosphorylated form 2 (Cx43-P2) were identified from the bottom up (Fig. 10A). TGF-β1 (5 ng/ml) application for 48 h significantly enhanced Cx43 abundance in cell lysates (+66%, $p < 0.001$; Fig. 10A). Single treatment of 18β-GA (25 µM) for 48 h or its simultaneous application with TGF-β1 induced no change in abundance of total Cx43. However, the addition of 18β-GA led to dephosphorylation of Cx43, as demonstrated by significant decrease of the Cx43-P2 band. This effect of 18β-GA was considered to be related to its function as a gap junction inhibitor.[25] In the parallel experiments, the SL-DT assay was performed to evaluate gap junction-mediated intercellular communication. TGF-β1 induced a broader area of LY migration than the vehicle, indicating that GJIC among TK 173 cells was significantly increased under TGF-β1 stimulation (+99%, $p < 0.001$; Fig. 10B). Single administration of 18β-GA alone or its combination with TGF-β1 abolished spread of LY between the TK 173 cells (-72% and -70% respectively, $p < 0.001$; Fig. 10B).

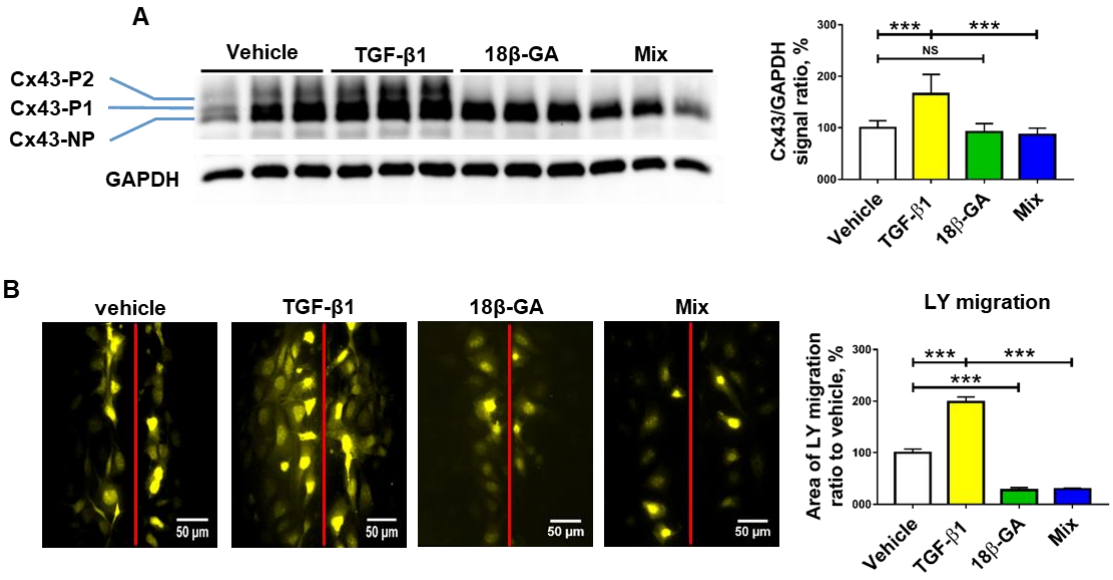

Figure 10. Effects of TGF-β1 and 18β-GA on Cx43 expression and gap junctional intercellular communication of cultured TK 173 cells. (A) The representative immunoblot shows Cx43 bands from TK 173 cell lysates treated with vehicle, TGF-β1 (5 ng/ml), 18β-GA (25 µM) or TGF-β1 + 18β-GA (Mix) for 48 h. GAPDH serves as the loading control. Densitometric evaluation of Cx43-immunoreactive bands is shown on the right. (B) Representative fluorescent images show migration of Lucifer yellow (LY) between

TK 173 cells treated with vehicle, TGF-β1, 18β-GA or Mix for 48 h. Quantification of LY migration areas is shown on the right. ***P < 0.001. NS, not significant. Figure 10 was obtained with permission from Yan Xu et al. 2021, Am J Physiol Renal Physiol, article PMID: 33196322 and is presented with modifications.[21]

4.10 Gap junctional coupling is involved in TGF-β1-induced activation of fibroblasts

Considering that TGF-β1 is the main profibrotic cytokine driving the progress of renal interstitial fibrosis, here we assumed that enhanced intercellular communication mediated by Cx43-positive gap junctions may play a role in myogenic transformation of fibroblasts induced by TGF-β1 signaling. For this purpose, α-SMA and Col1A1 expression by the TK 173 cells were quantified under TGF-β1 (5 ng/ml) and/or 18β-GA (25 µM) treatment for 48 h. TGF-β1 stimulation significantly upregulated abundance of α-SMA protein (2.3-fold, $p < 0.001$; Fig. 11, A and B) and Col1A1 mRNA (1.7-fold, $p < 0.01$; Fig. 11C) respectively, whereas additional administration of 18β-GA abolished this response. The application of 18β-GA alone decreased expression of α-SMA protein and Col1A1 mRNA (-62% and -83% respectively, $p < 0.001$; Fig. 11, A, B, and C).

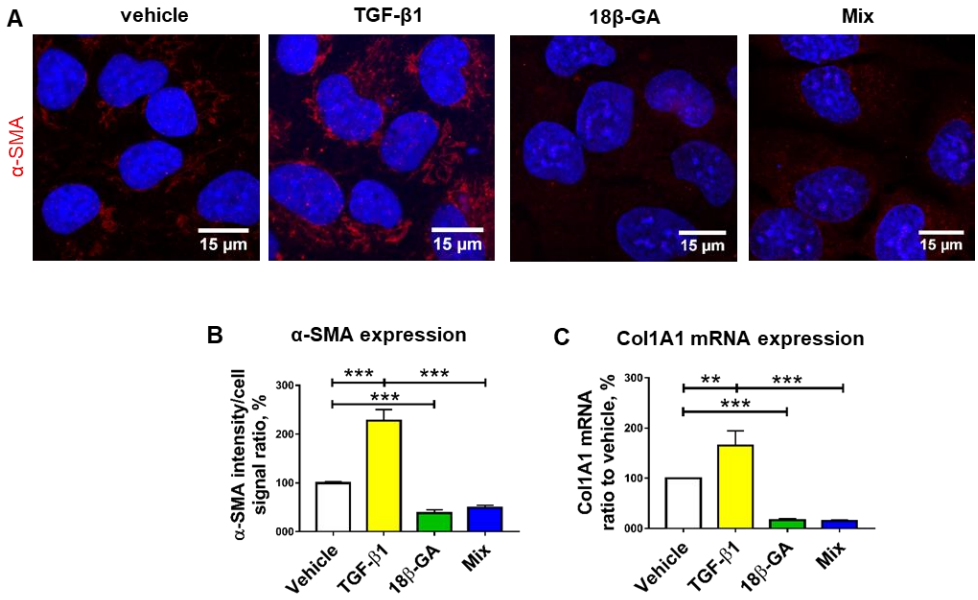

Figure 11. Effects of TGF-β1 and 18β-GA on myogenic transformation of cultured TK 173 cells. (A) Representative fluorescent images show migration of Lucifer yellow (LY) between TK 173 cells treated with vehicle, TGF-β1, 18β-GA or Mix for 48 h. (B) The graph shows quantification of signal intensities of α-SMA according to (A). (C) The graph shows Col1a1 mRNA quantity expressed by TK 173 cells treated with vehicle, TGF-β1, 18β-GA or Mix. **P < 0.01, ***P < 0.001. Figure 11 was obtained with permission from Yan Xu et al. 2021, Am J Physiol Renal Physiol, article PMID: 33196322 and is presented with modifications.[21]

5. Discussion

Gap junctions between endothelial cells of renal arteries and arterioles were detected using the freeze-fracture technique before.[26] Gap junctional coupling in arterial vasculature functions as the intercellular medium permitting propagation of action potentials between cells, thereby coordinating contraction of the arteries to work in concert.[27,28] Our results confirmed Cx43 distribution between endothelial cells of arcuate arteries, interlobular arteries, glomerular arterioles, peritubular capillaries, and descending vasa recta in rat and mouse kidney.[21] The glomerular capillaries, ascending thin limbs, inner medullary capillaries, and veins were Cx43-negative. Earlier findings have shown in part similar patterns,[10,11,28] however, some discrepancies need to be mentioned. Barajas et al. detected Cx43 in the media of renal arteries but not in endothelia,[9] which is controversial to most of relevant reports. In that study, a polyclonal antibody against the C-terminus of Cx43 was used, however, its specificity was not tested. Double labelling of Cx43 with CD31, an endothelial marker, in this study confirmed that Cx43 was strictly confined to the endothelium. Cx43 expression inside the glomerulus was described as endothelial signals by some researchers,[11] while others suggested that it was probably localized in mesangial cells.[29] Here, based on double labelling of Cx43 with CD31, intraglomerular Cx43 signals were not present in the endothelium. Zhang et al. reported distribution of Cx43 in the endothelium of isolated descending vasa recta, structurally confirmed by us, which participated in the spread of depolarization potentials induced by voltage clamp and in cytoplasmic Ca^{2+} response induced by luminal pressurization.[28] In our hands, Cx43 immunoreactivity was completely negative in the media of blood vessels except for signals grouped around granular cells. Although weaker than Cx40 and Cx37 expression, the presence of Cx43 around renin-producing cells was also detected by previous studies.[29,30] In a transgenic mouse model of granular cell-specific Cx43 deletion, renin mRNA, plasma renin activity, and systolic blood pressure did not differ significantly from wild-type mice,[29] probably due to compensation from other types of Cxs at this site. Mesangium is rich in gap junctional connections as observed by TEM,[12] likely to promote the propagation of calcium waves in the juxtaglomerular apparatus triggered by tubuloglomerular feedback in response to an increased tubular flow.[14] We found substantial Cx43 expression in the extraglomerular mesangium, which continued to be positive in the intraglomerular mesangium. These results extended findings of earlier localization studies.[9,31] A few researchers reported punctate Cx43

signals in the cytoplasm of inner medullary collecting ducts in rat kidney,[9] however, the majority of studies did not support this finding.

In our hands, the detection of medullary Cx43 signals within the interstitium was novel. Fibroblasts are the dominant cell type in the medullary interstitium. Fibroblasts with extensive cell processes form meshworks filling the space between renal epithelia and vasculature.[32,33] They have been known to show significant heterogeneity in structure and function.[32,33] Inner medullary fibroblasts bridge the interstitial space with their cell bodies vertical to the longitudinal axis of tubules and vessels like a ladder, and they are physically anchored to basement membranes of the thin limbs and capillaries by their processes or, sometimes, by their cell bodies.[34] An earlier scanning EM study reported that adjacent fibroblasts often contact with each other via their cell bodies or short processes.[33] The identity of Cx43-positive fibroblasts was confirmed by double immunostaining with COX-2, which was exclusively expressed by fibroblasts of inner medulla.[35] The absence of co-localization of Cx43 with tubular or capillary markers (AQP-1, AQP-2, CD31, and ZO-1) excluded the possibility of Cx43 distribution in these structures. In addition, immunogold labelling for Cx43 on ultrathin sections confirmed the finding ultrastructurally; Cx43 immunoreactivity was assigned to gap junctional areas between lipid-laden cells and between their processes. The results were supported by early morphological studies on renomedullary interstitial cells (inner medullary fibroblasts) analyzed by freeze-fracture technique; here, authors found gap junctions of variable size between isolated cell processes and between cell bodies of neighboring fibroblasts.[16,17] Consistent with our observation, junctions between fibroblast cell processes was more frequent than between their cell bodies.[21] Reflexive gap junctions with unclear function, formed through interaction of invaginated membranes from individual fibroblasts,[17] were Cx43-positive as well, suggesting functional reserves or communication between cell compartments.

The production and deposition of extracellular matrix is an important function of interstitial cells. Under pathological stimulation of profibrotic factors, resident fibroblasts are activated into myofibroblasts with highly expressed α-SMA and procollagen I driving the development of interstitial fibrosis.[36] This may cause uncontrolled tissue damage and renal dysfunction. Until now, the disease is incurable due to the lack of effective therapeutic interventions. Recently, several new targets for the treatment of renal fibrosis were identified including Cx43, discoidin domain receptor 1, periostin, and cannabinoid receptor 1.[20] However, whether Cx43-gap junctions play a role in myogenic

transformation of fibroblasts is still unknown. To address this, cultured human renal medullary fibroblasts (TK 173 cells) served us as a vitro model. Under stimulation of TGF-β1, the major profibrotic cytokine,[37] TK 173 cells upregulated α-SMA and Col1A1 expression along with enhanced Cx43 biosynthesis and GJIC. However, TGF-β1 failed to induce overexpression of α-SMA and Col1A1 upon gap junction blockade with the inhibitor 18β-GA, demonstrating that transduction of signaling in myofibroblast differentiation induced by TGF-β1 is dependent on Cx43-GJs. In consequence, only binding to its receptor may not be sufficient for TGF-β1 to stimulate activation of fibroblasts and matrix production by the cells; the reaction rather depends on increased cell-to-cell communication via gap junctions. The underlying mechanism probably involves in signal transduction through Cx43-GJs which regulates the expression of α-SMA and Col1A1. The results also suggest protective effects of reducing gap junctional exchange during development of renal interstitial fibrosis. Reduced α-SMA and Col1A1 synthesis upon application of 18β-GA alone indicated that gap junctions participate in the maintenance for physiological cell functions. An analogous investigation in cultured human bronchial fibroblasts showed similar results with α-SMA upregulation and Smad2 activation induced by TGF-β1, which were blunted after Cx43 knockdown.[38] The regulatory role of Cx43-GJs on TGF-β1 signaling and Col1 expression was also reported in other cell types. In cultured mouse cardiomyocytes, Cx43 was found to function as a positive regulator of the TGF-β signaling pathway via competition with Smad2/3 for microtubules binding, which means that the binding of Cx43 to microtubules may release Smads to the nucleus.[39] In osteoblasts, which are highly connected by Cx43-GJs, their inhibition downregulated transcription of Col1A1 gene through inactivating ERK signal pathway.[40]

In various mice models of experimental nephropathy Cx43 has been considered as a novel therapeutic target regarding the cure of chronic kidney disease (CKD).[19] Cx43 expression was enhanced in renal cortex of mice with CKD induced by hypertension or unilateral ureteral obstruction, while heterozygous knock-out of the gene or the use of antisense oligonucleotides administration significantly improved renal function and structures and diminished interstitial fibrosis.[19] In the same study, cultured mouse tubular cells were utilized as a corresponding *in vitro* model. Those cells expressed Cx43 gap junctions de novo under the stimulation of TGF-β1. The administration of Gap26, a specific Cx43-GJ blocker, blunted upregulation of Col1 mRNA expression by these cells

when induced by TGF-β1.[19] Consequently, Cx43 gap junctions were speculated to function as channels for exchange of second messengers related with Col1 transcription. In a similar study, mice with experimental glomerulonephritis achieved attenuation of crescent formation, interstitial fibrosis and other histopathologic changes upon heterozygous deletion of Cx43 or antisense oligonucleotides application.[41] Here, the authors found exacerbated ATP release and activation of purinergic signaling was associated with Cx43 upregulation induced by TGF-β1, resulting in profibrotic and proinflammatory responses.[41] In renal biopsies from patients with glomerulonephritis, abundant Cx43 immunoreactivity was detected in inflammatory cells, atrophic tubular cells, and interstitial cells in the damaged compartment.[42] In patients with severe nephroangiosclerosis or obstructive nephritis, Cx43 expression in glomerulus and interstitium was significantly increased compared to healthy controls.[19]

In the present study, our finding that profibrotic signaling between medullary fibroblasts was Cx43-GJ-dependent provides strong evidence for the suggestion that inhibition of Cx43 has a reno-protective effect in CKD. Considering upregulation of renal Cx43 in patients with various kidney diseases, the development of therapeutic approaches against increased Cx43 synthesis seems worthwhile for efforts in improving treatment for CKD.

Even though the inhibition of Cx43-GJs between cultured renal medullary fibroblasts prevented myogenic transformation, this effect needs further confirmation in animal models with activated fibroblasts and increased Cx43 expression in the kidney. Due to the limitation of access to normal kidney tissues from healthy individuals, Cx43 distribution in human kidney has not been fully revealed. Whether the anti-Cx43 therapy is effective and safe in patients with CKD needs to be addressed in future studies.

In conclusion, Cx43 was differentially localized in the renal vasculature and was abundantly expressed by medullary fibroblasts in the rodent kidneys, while it was absent in renal epithelium and veins. With respect to its function, our study found Cx43-GJs facilitate profibrotic signaling between medullary fibroblasts, which supports the recent finding that Cx43 is a potential therapeutic target in addressing renal fibrosis.

6. References

1. Kelly JJ, Simek J, Laird DW. Mechanisms linking connexin mutations to human diseases. *Cell Tissue Res.* 2015;360(3):701-721.
2. Koval M, Molina SA, Burt JM. Mix and match: investigating heteromeric and heterotypic gap junction channels in model systems and native tissues. *FEBS Lett.* 2014;588(8):1193-1204.
3. Ribeiro-Rodrigues TM, Martins-Marques T, Morel S, Kwak BR, Girao H. Role of connexin 43 in different forms of intercellular communication - gap junctions, extracellular vesicles and tunnelling nanotubes. *J Cell Sci.* 2017;130(21):3619-3630.
4. Stroemlund LW, Jensen CF, Qvortrup K, Delmar M, Nielsen MS. Gap junctions - guards of excitability. *Biochem Soc Trans.* 2015;43(3):508-512.
5. Soares AR, Martins-Marques T, Ribeiro-Rodrigues T, Ferreira JV, Catarino S, Pinho MJ, Zuzarte M, Isabel Anjo S, Manadas B, J PGS, Pereira P, Girao H. Gap junctional protein Cx43 is involved in the communication between extracellular vesicles and mammalian cells. *Sci Rep.* 2015;5:13243.
6. Wang X, Gerdes HH. Long-distance electrical coupling via tunneling nanotubes. *Biochim Biophys Acta.* 2012;1818(8):2082-2086.
7. Hanner F, Sorensen CM, Holstein-Rathlou NH, Peti-Peterdi J. Connexins and the kidney. *Am J Physiol Regul Integr Comp Physiol.* 2010;298(5):R1143-1155.
8. Solan JL, Lampe PD. Specific Cx43 phosphorylation events regulate gap junction turnover in vivo. *FEBS Lett.* 2014;588(8):1423-1429.
9. Barajas L, Liu L, Tucker M. Localization of connexin43 in rat kidney. *Kidney Int.* 1994;46(3):621-626.
10. Zhang J, Hill CE. Differential connexin expression in preglomerular and postglomerular vasculature: accentuation during diabetes. *Kidney Int.* 2005;68(3):1171-1185.
11. Takenaka T, Inoue T, Kanno Y, Okada H, Meaney KR, Hill CE, Suzuki H. Expression and role of connexins in the rat renal vasculature. *Kidney Int.* 2008;73(4):415-422.
12. Taugner R, Schiller A, Kaissling B, Kriz W. Gap junctional coupling between the JGA and the glomerular tuft. *Cell Tissue Res.* 1978;186(2):279-285.
13. De Vriese AS, Van de Voorde J, Lameire NH. Effects of connexin-mimetic peptides on nitric oxide synthase- and cyclooxygenase-independent renal vasodilation. *Kidney Int.* 2002;61(1):177-185.
14. Peti-Peterdi J. Calcium wave of tubuloglomerular feedback. *Am J Physiol Renal Physiol.* 2006;291(2):F473-480.

15. Stoessel A, Himmerkus N, Bleich M, Bachmann S, Theilig F. Connexin 37 is localized in renal epithelia and responds to changes in dietary salt intake. *Am J Physiol Renal Physiol.* 2010;298(1):F216-223.
16. Schiller A, Taugner R. Junctions between interstitial cells of the renal medulla: a freeze-fracture study. *Cell Tissue Res.* 1979;203(2):231-240.
17. Majack RA, Larsen WJ. The bicellular and reflexive membrane junctions of renomedullary interstitial cells: functional implications of reflexive gap junctions. *Am J Anat.* 1980;157(2):181-189.
18. Abed AB, Kavvadas P, Chadjichristos CE. Functional roles of connexins and pannexins in the kidney. *Cell Mol Life Sci.* 2015;72(15):2869-2877.
19. Abed A, Toubas J, Kavvadas P, Authier F, Cathelin D, Alfieri C, Boffa JJ, Dussaule JC, Chatziantoniou C, Chadjichristos CE. Targeting connexin 43 protects against the progression of experimental chronic kidney disease in mice. *Kidney Int.* 2014;86(4):768-779.
20. Prakoura N, Hadchouel J, Chatziantoniou C. Novel Targets for Therapy of Renal Fibrosis. *J Histochem Cytochem.* 2019;67(9):701-715.
21. Xu Y, Hu J, Yilmaz DE, Bachmann S. Connexin43 is differentially distributed within renal vasculature and mediates profibrotic differentiation in medullary fibroblasts. *Am J Physiol Renal Physiol.* 2021;320(1):F17-F30.
22. Brehm R, Zeiler M, Ruttinger C, Herde K, Kibschull M, Winterhager E, Willecke K, Guillou F, Lecureuil C, Steger K, Konrad L, Biermann K, Failing K, Bergmann M. A sertoli cell-specific knockout of connexin43 prevents initiation of spermatogenesis. *Am J Pathol.* 2007;171(1):19-31.
23. Muller GA, Frank J, Rodemann HP, Engler-Blum G. Human renal fibroblast cell lines (tFKIF and tNKF) are new tools to investigate pathophysiologic mechanisms of renal interstitial fibrosis. *Exp Nephrol.* 1995;3(2):127-133.
24. Upham BL, Sovadinova I, Babica P. Gap Junctional Intercellular Communication: A Functional Biomarker to Assess Adverse Effects of Toxicants and Toxins, and Health Benefits of Natural Products. *J Vis Exp.* 2016(118).
25. Guan X, Wilson S, Schlender KK, Ruch RJ. Gap-junction disassembly and connexin 43 dephosphorylation induced by 18 beta-glycyrrhetinic acid. *Mol Carcinog.* 1996;16(3):157-164.
26. Mink D, Schiller A, Kriz W, Taugner R. Interendothelial junctions in kidney vessels. *Cell Tissue Res.* 1984;236(3):567-576.
27. de Wit C, Roos F, Bolz SS, Pohl U. Lack of vascular connexin 40 is associated with hypertension and irregular arteriolar vasomotion. *Physiol Genomics.* 2003;13(2):169-177.

28. Zhang Q, Cao C, Mangano M, Zhang Z, Silldorff EP, Lee-Kwon W, Payne K, Pallone TL. Descending vasa recta endothelium is an electrical syncytium. *Am J Physiol Regul Integr Comp Physiol.* 2006;291(6):R1688-1699.
29. Gerl M, Kurt B, Kurtz A, Wagner C. Connexin 43 is not essential for the control of renin synthesis and secretion. *Pflugers Arch.* 2014;466(5):1003-1009.
30. Kurtz L, Janssen-Bienhold U, Kurtz A, Wagner C. Connexin expression in renin-producing cells. *J Am Soc Nephrol.* 2009;20(3):506-512.
31. Yao J, Morioka T, Li B, Oite T. Coordination of mesangial cell contraction by gap junction--mediated intercellular Ca(2+) wave. *J Am Soc Nephrol.* 2002;13(8):2018-2026.
32. Kaissling B, Le Hir M. Characterization and distribution of interstitial cell types in the renal cortex of rats. *Kidney Int.* 1994;45(3):709-720.
33. Takahashi-Iwanaga H. The three-dimensional cytoarchitecture of the interstitial tissue in the rat kidney. *Cell Tissue Res.* 1991;264(2):269-281.
34. Lemley KV, Kriz W. Anatomy of the renal interstitium. *Kidney Int.* 1991;39(3):370-381.
35. Campean V, Theilig F, Paliege A, Breyer M, Bachmann S. Key enzymes for renal prostaglandin synthesis: site-specific expression in rodent kidney (rat, mouse). *Am J Physiol Renal Physiol.* 2003;285(1):F19-32.
36. Kramann R, DiRocco DP, Humphreys BD. Understanding the origin, activation and regulation of matrix-producing myofibroblasts for treatment of fibrotic disease. *J Pathol.* 2013;231(3):273-289.
37. Meng XM, Nikolic-Paterson DJ, Lan HY. TGF-beta: the master regulator of fibrosis. *Nat Rev Nephrol.* 2016;12(6):325-338.
38. Paw M, Borek I, Wnuk D, Ryszawy D, Piwowarczyk K, Kmiotek K, Wojcik-Pszczola KA, Pierzchalska M, Madeja Z, Sanak M, Blyszczuk P, Michalik M, Czyz J. Connexin43 Controls the Myofibroblastic Differentiation of Bronchial Fibroblasts from Patients with Asthma. *Am J Respir Cell Mol Biol.* 2017;57(1):100-110.
39. Dai P, Nakagami T, Tanaka H, Hitomi T, Takamatsu T. Cx43 mediates TGF-beta signaling through competitive Smads binding to microtubules. *Mol Biol Cell.* 2007;18(6):2264-2273.
40. Stains JP, Civitelli R. Gap junctions regulate extracellular signal-regulated kinase signaling to affect gene transcription. *Mol Biol Cell.* 2005;16(1):64-72.
41. Kavvadas P, Abed A, Poulain C, Authier F, Labejof LP, Calmont A, Afieri C, Prakoura N, Dussaule JC, Chatziantoniou C, Chadjichristos CE. Decreased Expression of Connexin 43 Blunts the Progression of Experimental GN. *J Am Soc Nephrol.* 2017;28(10):2915-2930.
42. Hillis GS, Duthie LA, Brown PA, Simpson JG, MacLeod AM, Haites NE. Upregulation and co-localization of connexin43 and cellular adhesion molecules in inflammatory renal disease. *J Pathol.* 1997;182(4):373-379.

7. Statutory Declaration

“I, Yan Xu, by personally signing this document in lieu of an oath, hereby affirm that I prepared the submitted dissertation on the topic [Verteilung von Connexin 43 in der Säugerniere und seine Bedeutung bei der myogenen Transformation renomedullärer Fibroblasten; Distribution of connexin 43 in rodent kidney and its role in myogenic transformation of renal medullary fibroblasts], independently and without the support of third parties, and that I used no other sources and aids than those stated.

All parts which are based on the publications or presentations of other authors, either in letter or in spirit, are specified as such in accordance with the citing guidelines. The sections on methodology (in particular regarding practical work, laboratory regulations, statistical processing) and results (in particular regarding figures, charts and tables) are exclusively my responsibility.

Furthermore, I declare that I have correctly marked all of the data, the analyses, and the conclusions generated from data obtained in collaboration with other persons, and that I have correctly marked my own contribution and the contributions of other persons (cf. declaration of contribution). I have correctly marked all texts or parts of texts that were generated in collaboration with other persons.

My contributions to any publications to this dissertation correspond to those stated in the below joint declaration made together with the supervisor. All publications created within the scope of the dissertation comply with the guidelines of the ICMJE (International Committee of Medical Journal Editors; www.icmje.org) on authorship. In addition, I declare that I shall comply with the regulations of Charité – Universitätsmedizin Berlin on ensuring good scientific practice.

I declare that I have not yet submitted this dissertation in identical or similar form to another Faculty.

The significance of this statutory declaration and the consequences of a false statutory declaration under criminal law (Sections 156, 161 of the German Criminal Code) are known to me.”

Date Signature

8. Declaration of individual contribution to publication

Yan Xu has contributed to this publication:

Xu Y, Hu J, Yilmaz DE, Bachmann S. Connexin43 is differentially distributed within renal vasculature and mediates profibrotic differentiation in medullary fibroblasts. Am J Physiol Renal Physiol. 2021 Jan 1;320(1):F17-F30. doi: 10.1152/ajprenal.00453.2020. Epub 2020 Nov 16. PMID: 33196322. *Impact Factors 2019: 3.144*

Yan Xu is the sole first author. She conceived and designed this study under guidance of Prof. Sebastian Bachmann. She performed immunohistochemistry on tissue sections, immunocytochemistry, Western blotting, and quantitative rt-PCR. Scalpel Loading-Fluorescent Dye assay was done with the help of Junda Hu and cells were cultured with the help of Duygu Elif Yilmaz. Yan photographed the sections, analyzed all data, and interpreted results of the experiments. She further prepared all figures (Figure 1-7, supplemental Figure 1, 2) and the table (supplemental Table 1). She also wrote the methods and results parts and revised the final draft.

_____

Signature, date and stamp of first supervising university professor / lecturer

_____

Signature of doctoral candidate

9. Journal Data Filtered By: Selected JCR Year: 2019 Selected Editions: SCIE Selected Categories: 'PHYSIOLOGY' Selected Category Scheme: WoS

Journal Data Filtered By: **Selected JCR Year: 2019** Selected Editions: SCIE,SSCI
Selected Categories: **"PHYSIOLOGY"** Selected Category Scheme: WoS
Gesamtanzahl: 81 Journale

Rank	Full Journal Title	Total Cites	Journal Impact Factor	Eigenfactor Score
1	PHYSIOLOGICAL REVIEWS	28,712	25.588	0.024010
2	Annual Review of Physiology	9,466	19.556	0.010190
3	JOURNAL OF PINEAL RESEARCH	10,537	14.528	0.009430
4	PHYSIOLOGY	3,583	7.212	0.005380
5	International Journal of Behavioral Nutrition and Physical Activity	11,154	6.714	0.018870
6	Comprehensive Physiology	4,877	6.604	0.009170
7	JOURNAL OF CELLULAR PHYSIOLOGY	26,456	5.546	0.024290
8	Acta Physiologica	5,106	5.542	0.008320
9	EXERCISE AND SPORT SCIENCES REVIEWS	3,290	4.915	0.002720
10	Reviews of Physiology Biochemistry and Pharmacology	805	4.700	0.000670
11	JOURNAL OF PHYSIOLOGY-LONDON	50,045	4.547	0.037090
12	AMERICAN JOURNAL OF PHYSIOLOGY-LUNG CELLULAR AND MOLECULAR PHYSIOLOGY	13,085	4.406	0.015510
13	AMERICAN JOURNAL OF PHYSIOLOGY-HEART AND CIRCULATORY PHYSIOLOGY	26,114	3.864	0.020400
14	AMERICAN JOURNAL OF PHYSIOLOGY-GASTROINTESTINAL AND LIVER PHYSIOLOGY	14,186	3.725	0.012280
15	PSYCHOPHYSIOLOGY	14,586	3.692	0.012670
16	JOURNAL OF GENERAL PHYSIOLOGY	7,476	3.628	0.007380
17	International Journal of Sports Physiology and Performance	5,072	3.528	0.009760

Rank	Full Journal Title	Total Cites	Journal Impact Factor	Eigenfactor Score
18	AMERICAN JOURNAL OF PHYSIOLOGY-CELL PHYSIOLOGY	15,502	3.485	0.010450
19	AMERICAN JOURNAL OF PHYSIOLOGY-ENDOCRINOLOGY AND METABOLISM	18,917	3.469	0.013710
20	Frontiers in Physiology	21,190	3.367	0.052500
21	JOURNAL OF MAMMARY GLAND BIOLOGY AND NEOPLASIA	1,951	3.293	0.001080
22	CLINICAL JOURNAL OF SPORT MEDICINE	4,242	3.165	0.005100
23	PFLUGERS ARCHIV-EUROPEAN JOURNAL OF PHYSIOLOGY	9,355	3.158	0.009810
24	AMERICAN JOURNAL OF PHYSIOLOGY-RENAL PHYSIOLOGY	16,035	3.144	0.017010
25	JOURNAL OF BIOLOGICAL RHYTHMS	3,258	3.122	0.003220
26	JOURNAL OF APPLIED PHYSIOLOGY	43,194	3.044	0.020180
27	AMERICAN JOURNAL OF PHYSIOLOGY-REGULATORY INTEGRATIVE AND COMPARATIVE PHYSIOLOGY	17,896	2.992	0.013690
28	Journal of Physiological Sciences	1,380	2.955	0.002160
29	JOURNAL OF PHYSIOLOGY AND BIOCHEMISTRY	1,854	2.952	0.002340
30	PESTICIDE BIOCHEMISTRY AND PHYSIOLOGY	5,930	2.751	0.005660
31	PHYSIOLOGICAL GENOMICS	4,535	2.749	0.004520
32	INTERNATIONAL JOURNAL OF BIOMETEOROLOGY	6,418	2.680	0.007220
33	JOURNAL OF PHYSIOLOGY AND PHARMACOLOGY	3,342	2.644	0.002740
34	INTERNATIONAL JOURNAL OF PSYCHOPHYSIOLOGY	8,822	2.631	0.009440
35	EUROPEAN JOURNAL OF APPLIED PHYSIOLOGY	16,418	2.580	0.012130

Selected JCR Year: 2019; Selected Categories: “PHYSIOLOGY”

Rank	Full Journal Title	Total Cites	Journal Impact Factor	Eigenfactor Score
36	ARCHIVES OF PHYSIOLOGY AND BIOCHEMISTRY	1,104	2.575	0.001010
37	Conservation Physiology	1,342	2.570	0.004180
38	NEUROPHYSIOLOGIE CLINIQUE-CLINICAL NEUROPHYSIOLOGY	1,385	2.553	0.001770
39	Applied Physiology Nutrition and Metabolism	5,955	2.522	0.010250
40	CHRONOBIOLOGY INTERNATIONAL	5,708	2.486	0.006600
41	CLINICAL AND EXPERIMENTAL PHARMACOLOGY AND PHYSIOLOGY	5,813	2.456	0.004650
42	EXPERIMENTAL PHYSIOLOGY	5,710	2.431	0.006580
43	PHYSIOLOGICAL MEASUREMENT	6,066	2.309	0.006240
44	CRYOBIOLOGY	4,661	2.283	0.003850
45	CHEMICAL SENSES	4,553	2.261	0.003220
46	PHYSIOLOGICAL AND BIOCHEMICAL ZOOLOGY	3,033	2.250	0.002650
47	JOURNAL OF INSECT PHYSIOLOGY	9,006	2.246	0.006520
48	FISH PHYSIOLOGY AND BIOCHEMISTRY	4,825	2.242	0.004130
49	JOURNAL OF NEUROPHYSIOLOGY	40,570	2.225	0.032060
50	QUARTERLY JOURNAL OF EXPERIMENTAL PSYCHOLOGY	5,922	2.077	0.010080
51	Journal of Comparative Physiology B-Biochemical Systems and Environmental Physiology	3,768	2.042	0.002830
52	COMPARATIVE BIOCHEMISTRY AND PHYSIOLOGY A-MOLECULAR & INTEGRATIVE PHYSIOLOGY	10,391	1.966	0.005190
53	CANADIAN JOURNAL OF PHYSIOLOGY AND PHARMACOLOGY	4,900	1.946	0.003990
54	KIDNEY & BLOOD PRESSURE RESEARCH	1,903	1.898	0.003130

Selected JCR Year: 2019; Selected Categories: “PHYSIOLOGY”

Rank	Full Journal Title	Total Cites	Journal Impact Factor	Eigenfactor Score
55	JOURNAL OF MEMBRANE BIOLOGY	3,765	1.877	0.002400
56	KOREAN JOURNAL OF PHYSIOLOGY & PHARMACOLOGY	1,076	1.805	0.001780
57	HYPERTENSION IN PREGNANCY	1,314	1.787	0.001450
58	JOURNAL OF ELECTROMYOGRAPHY AND KINESIOLOGY	5,312	1.740	0.004060
59	Journal of Physiological Anthropology	826	1.730	0.000980
60	JOURNAL OF VASCULAR RESEARCH	1,551	1.725	0.001150
61	CLINICAL PHYSIOLOGY AND FUNCTIONAL IMAGING	2,409	1.704	0.003340
62	JOURNAL OF MUSCULOSKELETAL & NEURONAL INTERACTIONS	1,611	1.660	0.001490
63	PHYSIOLOGICAL RESEARCH	3,598	1.655	0.003680
64	RESPIRATORY PHYSIOLOGY & NEUROBIOLOGY	6,495	1.591	0.004210
65	ARCHIVES OF INSECT BIOCHEMISTRY AND PHYSIOLOGY	1,973	1.536	0.001230
66	ADVANCES IN PHYSIOLOGY EDUCATION	1,634	1.534	0.001620
67	JOURNAL OF COMPARATIVE PHYSIOLOGY A-NEUROETHOLOGY SENSORY NEURAL AND BEHAVIORAL PHYSIOLOGY	5,007	1.516	0.003390
68	JOURNAL OF BIOLOGICAL REGULATORS AND HOMEOSTATIC AGENTS	1,924	1.506	0.002820
69	Lymphatic Research and Biology	860	1.492	0.001130
70	PEDIATRIC EXERCISE SCIENCE	1,987	1.489	0.002220
71	Physiology International	137	1.410	0.000280
72	CHINESE JOURNAL OF PHYSIOLOGY	575	1.151	0.000480

Rank	Full Journal Title	Total Cites	Journal Impact Factor	Eigenfactor Score
73	GENERAL PHYSIOLOGY AND BIOPHYSICS	958	1.070	0.000890
74	BIOLOGICAL RHYTHM RESEARCH	816	0.826	0.000860
75	CRYOLETTERS	925	0.702	0.000610
76	ZHURNAL VYSSHEI NERVNOI DEYATELNOSTI IMENI I P PAVLOVA	305	0.432	0.000110
77	JOURNAL OF EVOLUTIONARY BIOCHEMISTRY AND PHYSIOLOGY	371	0.382	0.000230
78	NEUROPHYSIOLOGY	232	0.322	0.000200
79	Revista Brasileira de Medicina do Esporte	792	0.309	0.000290
80	LYMPHOLOGY	791	0.233	0.000490
81	KLINISCHE NEUROPHYSIOLOGIE	54	0.111	0.000010

10. Manuscript of the publication

Xu Y, Hu J, Yilmaz DE, Bachmann S. Connexin43 is differentially distributed within renal vasculature and mediates profibrotic differentiation in medullary fibroblasts. Am J Physiol Renal Physiol. 2021 Jan 1;320(1):F17-F30. doi: 10.1152/ajprenal.00453.2020. Epub 2020 Nov 16. PMID: 33196322. *Impact Factors 2019: 3.144*

Publication: Connexin43 is differentially distributed within renal vasculature and mediates profibrotic differentiation in medullary fibroblasts

Xu Y, Hu J, Yilmaz DE, Bachmann S. Am J Physiol Renal Physiol. 2021 Jan 1;320(1):F17-F30.

https://doi.org/10.1152/ajprenal.00453.2020

Publication: Connexin43 is differentially distributed within renal vasculature and mediates profibrotic differentiation in medullary fibroblasts

Xu Y, Hu J, Yilmaz DE, Bachmann S. Am J Physiol Renal Physiol. 2021 Jan 1;320(1):F17-F30.

https://doi.org/10.1152/ajprenal.00453.2020

Publication: Connexin43 is differentially distributed within renal vasculature and mediates profibrotic differentiation in medullary fibroblasts

Xu Y, Hu J, Yilmaz DE, Bachmann S. Am J Physiol Renal Physiol. 2021 Jan 1;320(1):F17-F30.

https://doi.org/10.1152/ajprenal.00453.2020

Publication: Connexin43 is differentially distributed within renal vasculature and mediates profibrotic differentiation in medullary fibroblasts

Xu Y, Hu J, Yilmaz DE, Bachmann S. Am J Physiol Renal Physiol. 2021 Jan 1;320(1):F17-F30.

https://doi.org/10.1152/ajprenal.00453.2020

Publication: Connexin43 is differentially distributed within renal vasculature and mediates profibrotic differentiation in medullary fibroblasts

Xu Y, Hu J, Yilmaz DE, Bachmann S. Am J Physiol Renal Physiol. 2021 Jan 1;320(1):F17-F30.

https://doi.org/10.1152/ajprenal.00453.2020

Publication: Connexin43 is differentially distributed within renal vasculature and mediates profibrotic differentiation in medullary fibroblasts

Xu Y, Hu J, Yilmaz DE, Bachmann S. Am J Physiol Renal Physiol. 2021 Jan 1;320(1):F17-F30.

https://doi.org/10.1152/ajprenal.00453.2020

Publication: Connexin43 is differentially distributed within renal vasculature and mediates profibrotic differentiation in medullary fibroblasts

Xu Y, Hu J, Yilmaz DE, Bachmann S. Am J Physiol Renal Physiol. 2021 Jan 1;320(1):F17-F30.

https://doi.org/10.1152/ajprenal.00453.2020

Publication: Connexin43 is differentially distributed within renal vasculature and mediates profibrotic differentiation in medullary fibroblasts

Xu Y, Hu J, Yilmaz DE, Bachmann S. Am J Physiol Renal Physiol. 2021 Jan 1;320(1):F17-F30.

https://doi.org/10.1152/ajprenal.00453.2020

Publication: Connexin43 is differentially distributed within renal vasculature and mediates profibrotic differentiation in medullary fibroblasts

Xu Y, Hu J, Yilmaz DE, Bachmann S. Am J Physiol Renal Physiol. 2021 Jan 1;320(1):F17-F30.

https://doi.org/10.1152/ajprenal.00453.2020

Publication: Connexin43 is differentially distributed within renal vasculature and mediates profibrotic differentiation in medullary fibroblasts

Xu Y, Hu J, Yilmaz DE, Bachmann S. Am J Physiol Renal Physiol. 2021 Jan 1;320(1):F17-F30.

https://doi.org/10.1152/ajprenal.00453.2020

Publication: Connexin43 is differentially distributed within renal vasculature and mediates profibrotic differentiation in medullary fibroblasts

Xu Y, Hu J, Yilmaz DE, Bachmann S. Am J Physiol Renal Physiol. 2021 Jan 1;320(1):F17-F30.

https://doi.org/10.1152/ajprenal.00453.2020

Publication: Connexin43 is differentially distributed within renal vasculature and mediates profibrotic differentiation in medullary fibroblasts

Xu Y, Hu J, Yilmaz DE, Bachmann S. Am J Physiol Renal Physiol. 2021 Jan 1;320(1):F17-F30.

https://doi.org/10.1152/ajprenal.00453.2020

Publication: Connexin43 is differentially distributed within renal vasculature and mediates profibrotic differentiation in medullary fibroblasts

Xu Y, Hu J, Yilmaz DE, Bachmann S. Am J Physiol Renal Physiol. 2021 Jan 1;320(1):F17-F30.

https://doi.org/10.1152/ajprenal.00453.2020

Publication: Connexin43 is differentially distributed within renal vasculature and mediates profibrotic differentiation in medullary fibroblasts

Xu Y, Hu J, Yilmaz DE, Bachmann S. Am J Physiol Renal Physiol. 2021 Jan 1;320(1):F17-F30.

https://doi.org/10.1152/ajprenal.00453.2020

11. Curriculum Vitae

My curriculum vitae does not appear in the electronic version of my paper for reasons of data protection

My curriculum vitae does not appear in the electronic version of my paper for reasons of data protection

My curriculum vitae does not appear in the electronic version of my paper for reasons of data protection

12. Complete list of publications

1. **Xu Y**, Hu J, Yilmaz DE, Bachmann S. Connexin43 is differentially distributed within renal vasculature and mediates profibrotic differentiation in medullary fibroblasts. Am J Physiol Renal Physiol. 2021 Jan 1;320(1):F17-F30. doi: 10.1152/ajprenal.00453.2020. Epub 2020 Nov 16. PMID: 33196322. *Impact Factors 2019: 3.144*

2. Hu J, **Xu Y**, Bachmann S, Mutig K. Angiotensin II receptor blockade alleviates calcineurin inhibitor nephrotoxicity by restoring cyclooxygenase 2 expression in kidney cortex. Acta Physiol (Oxf). 2020 Dec 29:e13612. doi: 10.1111/apha.13612. Epub ahead of print. PMID: 33377278. *Impact Factors 2019: 5.542*

13. Acknowledgements

I would like to thank my supervisor Prof. Dr. Sebastian Bachmann who gave me the opportunity to study here and guided me in the field of nephrology. He helped a lot in my doctoral project. I learned how to use different microscopies and how to evaluate immunohistochemistry results from him, which are very important for basic research. In addition, I would like to thank my second supervisor PD. Dr. Kerim Mutig, who was always friendly and kindly to help. He offered creative ideas to improve my study. Besides, I want to thank my colleagues, Anette Drobbe, Junda Hu, Duygu Elif Yilmaz, Hasan Demirci, Suncica Popovic as well. They were all very friendly and nice to me. We collaborated very well to move the project forward. Furthermore, I want to thank Kerstin Riskowsky, John Horn, Petra Schrade, and Katja Dörfel. They taught me research protocols and sharpened my techniques.